Entropic contribution of lattice cluster theory for short chain isomers

Gottfried Segner, B.Sc.

Graz, May 2020

Entropic contribution of lattice cluster theory for short chain isomers

Master thesis

to obtain the degree of

Master of Science

in

Chemical Engineering

submitted to the

Graz University of Technology

Coordinator:

Dr.-Ing. Patrick Zimmermann M.Sc.

Institute of Chemical Engineering and Environmental Technology

Graz, May 2020

EIDESSTATTLICHE ERKLÄRUNG

Ich erkläre an Eides statt, dass ich die vorliegende Arbeit selbstständig verfasst, andere als die angegebenen Quellen/Hilfsmittel nicht benutzt, und die den benutzten Quellen wörtlich und inhaltlich entnommenen Stellen als solche kenntlich gemacht habe.

Graz, am ………………………… ………………………………………

(Unterschrift)

STATUTORY DECLARATION

I declare that I have authored this thesis independently, that I have not used other than the declared sources / resources, and that I have explicitly marked all material which has been quoted either literally or by content from the used sources.

Graz, ……………………… ………………………………………

date (signature)

Kurzfassung

Isomere sind ein bedeutendes Forschungsfeld in der heutigen chemischen Industrie. Reine Isomere sind schwer zum Gewinnen, da sich die Eigenschaften der Isomere stark ähneln. Dies macht eine Theorie, um deren Eigenschaften vorauszusagen umso bedeutender.

Die „Lattice Cluster Theorie" (LCT) (1) (2) eignet sich gut zur Beschreibung der thermodynamischen Eigenschaften von Polymeren. Sie bestimmt Eigenschaften über das Berechnen der Zustandssumme eines Systems. Durch eine zweifache Reihenentwicklung in der Gitterkoordinationsnummer z und der molekularen Interaktionsenergie ε liefert sie einen Ausdruck für die freie Helmholtz Energie. Die Flory Huggins Theorie dient dabei als „mean field", welches von einer unverzweigten Kette ausgeht. Einflüsse der Architektur des Isomers korrigieren dann einzelne Beiträge der Strukturen, die man im Molekül findet. Die bisherige Theorie beachtet dafür Strukturdiagramme mit bis zu vier Bindungen, sowie bis zu zwei Wechselwirkungen, welche jeweils eine Bindung ersetzten. Was Beiträgen einer Ordnung von bis zu $\varepsilon^2 z^{-2}$ entspricht. Ihre große Stärke liegt darin, dass sie basierend auf einem Parameterset in der Lage ist, die thermodynamischen Eigenschaften der anderen Isomere zu beschreiben. In ihrer inkompressiblen Form konnte die LCT bereits unter anderem für Polystyrol Mischungen (3), Copolymere (4) und hochverzweigte Polymere (5) angewendet werden. Leider stößt die LCT bei kurzkettigen Kohlenwasserstoffen in ihrer aktuellen Form an ihre Grenzen. Die Betrachtung von Beiträgen mit der Ordnung von bis zu z^{-3} verbessert jedoch die Anwendbarkeit der LCT auf diese (6).

Daraus ergibt sich als nächster Schritt das Erweitern jener auf ε^3. Die somit Diagramme mit bis zu sechs Bindungen berücksichtigen. Um den nötigen Aufwand zu minimieren sind vorerst nur entropische Diagramme berücksichtigt worden. Der energetische Anteil wurde über das „mean field" dargestellt. Durch den Vergleich einer berechneten Dampfdruckkurve mit experimentellen Werten, sollen die Auswirkungen der Erweiterung erkenntlich sein. Das hierdurch erweiterte Model ist in der Lage eindeutig zwischen den Isomeren zu unterscheiden, kann aber durch die fehlenden energetischen Diagramme noch keine exakten Ergebnisse liefern.

Abstract

Isomers are an important field of research in the present chemical industry. Purely branched substances are difficult to obtain because the properties of the isomers are very similar. This makes a theory to predict their properties even more important.

The Lattice Cluster Theory (LCT) (1) (2) is a useful tool to describe the thermodynamic properties of polymers. It derives properties by determining the sum of states of a system. It delivers an expression for the Helmholtz energy by a twofold series development in the lattice coordination number z and the molecular interaction energy ε. The Flory Huggins theory serves as a mean field which assumes an unbranched chain. The architecture of the isomer then corrects this by adding individual contributions from the structures found in the molecule. The current theory considers structural diagrams with up to four bonds and up to two interactions, each replacing one bond. This corresponds to contributions of an order up to $\varepsilon^2 z^{-2}$. Its great strength is that it is able to describe the thermodynamic properties of the other isomers based on a set of parameters. In its incompressible form, LCT has already been used for polystyrene mixtures (3), copolymers (4) and highly branched polymers (5). Unfortunately, LCT reaches its limits with short-chain hydrocarbons in its current form. However, the consideration of contributions with up to z^{-3} improves the applicability of LCT to these (6).

The next step is the extension of the LCT to ε^3, which therefore considers diagrams with up to six bonds. To minimize the necessary effort, only entropic diagrams have been considered for the time being. The energetic part was represented by the mean field. By inspecting the vapour pressure curve derived from this adapted model compared to some experimental values, the effect of the extension should be noticeable. The adapted model can distinguish clearly between the isomers, but due to the missing energetic diagrams it is not yet able to give exact results.

Acknowledgement

"Peace cannot be kept by force; it can only be achieved by understanding."

— Albert Einstein

Table of content

1   Introduction

Isomers are chemical substances that have the same composition but a different structure. The term isomerism was established as early as 1830, when Liebig and Wöhler discovered silver fuliminate and silver cyanate (7). Both have different properties although they consist of the same composition of atoms. Isomerism can occur in many different forms and has significance in many technical areas. For example, mirror isomeric substances are of great importance in the pharmaceutical and biotechnological industry. Like many isomers, they have similar physical and chemical properties but, in their case, they differ greatly in their biological properties.

The separation of the individual isomers is made difficult by the generally very similar chemical and physical properties. Especially the isomers whose structure are alike can only be purified by extensive methods. This further leads to the measurement of such substance data to become expensive and difficult. Pure substance data about isomers are therefore rare. Only for the purification of the unbranched compounds a multitude of processes exist. For example, urea can be used in the Urea Extractive Crystallization process (8) to isolate them. Furthermore, the number of isomers increases exponentially with chain length (9). This can be observed well with the example of alkanes. While there are two different structures for butane, the number of theoretical isomers for decane is already 75 and for $C_{20}H_{22}$ there are theoretically 366319 different isomers. However, not all of them occur in nature due to steric hindrance. The analysis of so many different components is not feasible on a realistic scale.

For the design of many processes one must therefore resort to thermodynamic models and estimations to describe their properties. Many models cannot really distinguish between the individual isomers. By which they either reflect the properties of an unbranched substance or an average of the individual isomers. Other models may differ between them but require a separate parameter set for each isomer. To get such a parameter set one would need some experimental data. This limits their usage for some applications.

The Lattice Cluster Theory (LCT) (1) provides a useful tool capable of distinguishing many isomers. It is based on the Flory Huggins theory (FH) developed in 1953 (10). FH is one of the first models that could correctly describe the properties of polymeric solutions for many polymers. It considers polymers as chains of segments, which are placed on a lattice. By calculating all the way such a chain can be placed on the lattice it can calculate the constitutional entropy of the system. By further applying interaction forces between the chains, it arrives at an expression for the Helmholtz energy of the system, which can be used to describe a large amount of properties of the system. Many models stem from the FH to describe polymers even better. The FH only allows the modelling of unbranched substances. The LCT corrects this by using a cluster expansion that resembles Mayer's cluster (11) expansion for nonideal gases. It considers the FH as a mean field and by adding corrections, it can also be used for branched polymers. These corrections are derived from the structures found in the chain. It only requires one set of parameters for all isomers of a component. These can be easily obtained from the unbranched isomers.

It was originally developed to describe branched polymers, which in nature often appear as a spectrum for the degree of branching. Thanks to some improvements, it can also be used in its incompressible form for polystyrene blends (3), copolymers (4) and hyperbranched polymers (5) are used. Thanks to the introduction of empty lattices sites, so-called "voids", even compressible properties of polymers can be described. By considering these as separate non-interacting components (12), it could even be used for describing the vapour pressure long-chain alkanes.

In the case of shorter-chain hydrocarbons such as hexane, however, it unfortunately still reaches its limits. While it can predict the properties of the isomers of high chain hydrocarbons with considerable accuracy, it has difficulties in predicting the sequence of the isomers in the case of short chain hydrocarbons, for example in the case of vapour pressure. In its current form it can hardly distinguish between the isomers of short-chain hydrocarbons. This form of the model includes all diagram contributions that meet the following criteria, a lattice coordination number z with a minimum power raised to minus two and a number of bonds in the diagram of up to four bonds which correlates with a maximum power of the interaction parameter ε raised to two. All other diagram contributions are neglected, since their contribution becomes comparable small. In the case of short-chain ones, Zimmermann et al. (6)

found that the inclusion of diagram contributions with a minimum coordination number z of minus three significantly improves the predictive power of LCT for such. This enhancement enables it to distinguish between the individual short-chain isomers and even ranks their properties in the correct order. The calculated vapour pressures of the hexane isomers are still too close to those of the n-hexane used for parameter calibration. The next resulting step to extend the LCT is therefore to include diagram contributions from diagrams with up to six bonds. This corresponds to a maximum order of the interaction parameter of three. In order to demonstrate the possible effect of including these diagram contributions, this thesis will primarily examine the contribution of entropic diagrams. The energetic contributions are modelled only by the mean field contribution from the FH. The result of such an extension is then presented by comparison with experimental data and results from previous models.

2 Theory

The Lattice Cluster theory (LCT) (1) derives from the Flory Huggins theory (FH) (10) which stems from the statistic thermodynamic. However, FH Theory can also be seen as a special case of LCT, the case of unbranched molecules. In the case of unbranched molecules, FH Theory is able to describe the properties of polymer melts and solutions. It starts from a lattice in which the individual molecules are located. The individual polymer molecules are significantly larger than the molecules of the solvents. While the latter can be placed in a lattice site, this is not possible with the polymer molecules. Instead, the polymer molecule is divided into segments of the same order of magnitude as the lattice sites. These segments are then placed one after the other alongside each other in the lattice. The neighbouring sides where the next segment is located can be described by a statistical probability. This way the possible states of the system can be described. The entropy of a system is defined by the number of possible states it can have. This is expressed in the Boltzmann's equation Eq. 2.1. k_B is the Boltzmann constant and Z is the partition function of the system, which specifies its sum of states.

$$S = k_B \ln Z$$ **Eq. 2.1**

A state is a distinguishable microstate of the system. Two states are then distinguishable if at least one molecule has a different position, you can distinguish further if a molecule has another amount of energy, such as that which can be triggered by interaction forces. If two molecules of the same kind, with the same energy, are exchanged, the new state is indistinguishable from the before. The states are only counted as a single state. It is possible to obtain an expression of the Helmholtz Energy F by Eq. 2.2 through the sum of the microstates. With the help of this, one can describe a large set of the thermodynamic properties of a substance.

$$F = -k_B T \ln Z$$ **Eq. 2.2**

The FH theory is derived according to Dudowicz et al (3). The consideration of volume contraction ensures that no two segments of the chain share a lattice place. In the case of a two-segment chain in a 2x2 lattice, these can still just be counted. Figure 1 shows all possibilities for such a case
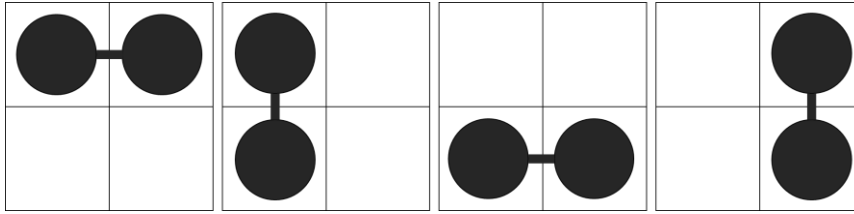
Figure 1: All possible configural states of a two segmented chain with identical segments in a 2x2 lattice

In a real example with long chains and huge spatial lattices, this is no longer possible. This is done mathematically by a several fold constrained sum (Eq. 2.3) (3)of the Kronecker delta δ over all segments of the chain, all placed chains, all lattice locations and all adjacent lattice locations. The Kronecker delta is a mathematical function that returns zero if the two input variables are different and one if they are equal. The restriction of the sum is denoted as S, which is the condition that no counter i is the same. In the sum k is the number of components in the system, n_μ is the number of chains of one component, N_μ is the number of segments in a chain, z is the coordination number, r is lattice position and α is a vector pointing to the adjacent positions. In the previous example the restricted sum would look like in equation Eq. 2.4.

$$Z = \prod_{\mu=1}^{k} \frac{1}{n_\mu! \, 2^{n_\mu}} \sum_S \prod_{m_\mu}^{n_\mu} \left\{ \prod_{\alpha_\mu=1}^{N_\mu-1} \sum_{\beta_{\alpha_\mu,m_\mu}^\mu=1}^{z} \delta\left(r_{i_{\alpha_\mu,m_\mu}^\mu}, r_{i_{\alpha_\mu+1,m_\mu}^\mu} + \alpha_{\beta_{\alpha_\mu,m_\mu}^\mu} \right) \right\} \qquad \textbf{Eq. 2.3}$$

$$Z = \prod_{\mu=1}^{1} \frac{1}{1! \, 2^1} \sum_{i_1 \neq i_2} \prod_{m_\mu}^{1} \left\{ \prod_{\alpha_\mu=1}^{1} \sum_{\beta_{\alpha_\mu,m_\mu}^\mu=1}^{4} \delta\left(r_{i_{\alpha_\mu,m_\mu}^\mu}, r_{i_{\alpha_\mu+1,m_\mu}^\mu} + \alpha_{\beta_{\alpha_\mu,m_\mu}^\mu} \right) \right\} = 4 \qquad \textbf{Eq. 2.4}$$

The energetic states of the system are then determined by the interaction energies. Repulsion forces are already considered as volume exclusion. Attractive forces are only considered if the two segments are located exactly next to each other. Seg-

ments that are further away from each other are considered to be non-interacting. The attractive forces can also be expressed as a several fold constrained sum of the Kronecker delta δ multiplied by the interaction parameter $\varepsilon_{1,2}$ in this case.

The FH theory involves some assumptions which limit its usage. It assumes that all lattice spaces not occupied by polymer chains are occupied by monomers. This results in the absence of free volume spaces. It further assumes that all molecules are far larger than the monomers and are branchless. FH ignores preferred orientations of the molecules, through its rudimentary description of attractive forces and only allows one kind of segment. These assumptions result in following limitations:

- The solvent is described by single segments
- The usable solvent is limited
- It only models incompressible systems
- It can`t describe isomers and branched polymers

The FH theory is therefore not usable for a lot of cases. In order to circumvent this limitation, the FH has been modified in several ways. One of these further developments is the Lattice Cluster Theory (LCT) of Freed and co-workers (1). This theory especially revises the assumption of unbranched chains.

The LCT thus corrects some of the assumptions of Flory Huggins by using ta cluster expansion approach like Mayer`s Cluster expansion for nonideal gases (11). It takes the entropic part of the Flory Huggins theory as a mean field and adds all the deviations as power series expansion. Each one of these added terms is a cluster diagram. A cluster diagram represents a structure which can be found in the molecular chain. This leads finally to the representation Eq. 2.5 for the state sum. Here Z^{MF} represents the state sum which results from the FH and C_{Bm} the contribution of an individual diagram.

$$Z = Z^{MF}\left(1 + \sum_{B} C_{Bm}\right)$$

Eq. 2.5

The diagrams can be divided into three different kinds.

- Diagrams of the first kind which consist of only one structure.
- Diagrams of the second kind which consist of the combination of two structures and are on two different molecules.
- Diagrams of the third kind which also consist of several structures but where two of them are at least on the same molecule.

Every Cluster diagram contribution is divisible into a lattice dependent and a combinatorial part. The lattice-dependent part is determined by volume contraction or the attraction of a diagram. It is completely independent of the architecture of the molecules but depends on the diagram structure and the properties of the lattice. The combinatorial part depends on the number of ways the Diagram can be found in the inspected molecules. The lattice has no influence on it. In order to determine the contribution of a diagram, these two parts must first be calculated. The new expression for the free energy, based on the new description for the sum of states, is now Eq. 2.6

$$F = -k_B T \, ln \left\{ Z^{MF} \left(1 + \sum_B D_B * \gamma_B \right) \right\}$$

<div align="right">**Eq. 2.6**</div>

It now contains the logarithm of a sum. This logarithm can be expanded into a Taylor series (Eq. 2.7). After expanding the individual terms of the sum, it can be rearranged in such a way that diagrams with the same composition of structures are always standing next to each other. The different ways in which a diagram can be represented are called cumulants. Diagrams of the first kind are made up of a single structure and only occur in the linear term in this rearranged series. For the other diagrams, the diagram contribution is now formed from the sum of the cumulants. Each of the cumulants has its own lattice dependent and combinatorial contribution. The calculation of the lattice dependent and the combinatorial part for these differs slightly between them. Cumulants that are composed of several smaller diagrams consist in separate units. In contrast to the main cumulant, which consists of only one diagram, these separate units do not restrict each other.

$$ln\left(1 + \sum_B D_B * \gamma_B\right) = \left(\sum_B D_B * \gamma_B\right) - \frac{1}{2} * \left(\sum_B D_B * \gamma_B\right)^2$$

$$+ \frac{1}{3} * \left(\sum_B D_B * \gamma_B\right)^3 \quad \text{....} \qquad\qquad\qquad \textbf{Eq. 2.7}$$

The lattice-dependent fraction D_B can also be expressed as Eq. 2.8. It is then composed of α and d_B. α is only dependent on the number of lattice locations in the lattice and the number of lattice sides that a diagram occupies. It is calculated with Eq. 2.9, where N_l is the number of lattice positions and k_c is the number of segments in the Diagram. d_B specifies the number of ways in which a diagram cannot be folded together due to volume exclusion and is represent as a restricted sum. This sum adds up over all lattice positions for each segment of the graph and for each bond over all directions, but no lattice position of a segment may be the same. This restricted sum can be represented by several unrestricted sums. The unrestricted sum over all lattice positions and orientations, minus all the sums representing cases where some segments share a lattice position. By applying graph theory, one can see that these cases can be represented by so-called contracted graphs. When a graph is contracted, two vertices of the graph are merged, and the edges of the vertices are transferred to the new vertex. In this case, a contracted vertex represents the sharing of a lattice space and is therefore a prohibited case. Each of these diagrams thus adds a contribution to d_B. Since a contracted diagram can usually be formed in several ways from an initial diagram, they cover several possible prohibited cases. Therefore, their contributions must be given a pre-factor to include all cases. The result is that d_B is described by the sum shown in Eq. 2.10. R_{Bm} is the contribution of one of the diagrams. By applying graph theory Brahznik (13) can list all significant contracted diagrams up to eight bonds and their contribution. Contracted diagrams that make no contribution because their contribution becomes zero in the thermodynamic limit were intentionally left out. The pre-factor f_{Bc} results from the number of possibilities to construct a contracted diagram and their number of merged vertices. In the case of the cumulants, it should be ensured that the separated entities of the cumulant are not connected to each other by merging the vertices. By determining the individual pre-

factors, the lattice-dependent contribution D_B can be calculated using the equations Eq. 2.8 and Eq. 2.10.

$$D_B = \frac{d_B}{\alpha}$$ **Eq. 2.8**

$$\alpha = N_l * (N_l - 1) * (N_l - 2) * ... * (N_l - k_c + 1)$$ **Eq. 2.9**

$$d_B = \sum_c f_{B,c} R_{B,c}$$ **Eq. 2.10**

The combinatorial fraction results from the structural form and the number of molecules. It indicates how often a diagram can be found in a system. This is achieved by placing the individual structures of a diagram one after the other on all possible positions in a molecule. With second and third kinds of diagrams, it is important that no segments are occupied twice, otherwise the diagram would be incomplete. With multi-component systems, it is more difficult because the individual structures of the diagrams can be located on the same or different components. All possible distributions of the structures must then be added together. For cumulants with separate entities, the restriction of the double assignment of segments does not apply. In this case, the individual entities are complete even if they share a segment with another entity.

By summing up the products of the combinatorial and lattice dependent fractions, the contribution of a diagram to the correction of the mean field is obtained for all cumulants. The thermodynamic limit, which in this case makes the number of lattice locations N_l in the lattice go towards infinity, causes any correction without N_l in the counter to be negligible. This significantly reduces the number of contributions and their number of terms. It even results in the fact that some diagrams, such as diagram 1a, have no contribution.

As with the FH theory, the interactions between the individual segments must be considered in LCT. This is not yet included in the mean field of the LCT, they are added as another kind of cluster diagrams instead. These energetic diagrams are like entropic diagrams except that some bonds have been replaced by energetic interactions. The contribution of the energetic mean field comes from the diagram with only

a single interaction bond. Its contribution results from the power series development of the underlying Mayer-f function Eq. 2.11.

$$f_{\mu\lambda} = e^{\varepsilon_{\mu\lambda}} - 1 = \varepsilon_{\mu\lambda} + \frac{\varepsilon_{\mu\lambda}^2}{2} + \frac{\varepsilon_{\mu\lambda}^3}{6} \ldots$$

Eq. 2.11

The contributions of the energetic cluster diagrams are obtained by Eq. 2.12. The D_{Be} stems from multiplying the lattice -dependent part D_B of an entropic diagram by the first term of the Taylor series development of the equation Eq. 2.13.

$$C_{Be} = D_{Be} * \gamma_D * s_D$$

Eq. 2.12

$$\left[\frac{\frac{f_{\mu\gamma}z}{N_l}}{1 + \frac{f_{\mu\gamma}z}{N_l}} \right]^l = \frac{z}{N_l} * \varepsilon_{\mu\lambda} \ldots$$

Eq. 2.13

For each replaced bond the contribution must be multiplied by the left hand side of Eq. 2.13. This is represented as the power l and results in the epsilon order of the model. The higher the power of the contribution, the more bonds were replaced by interaction bonds. s_D is the number of symmetries of the diagram. While γ_D represents the number of ways to select the bonds and vertices with interaction in the molecule. After applying the thermodynamic limit, the calculated energetic contributions are summed up after applying the thermodynamic limit and added to the expression Eq. 2.5 of the sum of states. Thus, the new expression for the sum of states is Eq. 2.14. Which results in a final expression for the Helmholtz energy F of Eq. 2.15.

$$Z = Z^{MF} \left(1 + \sum_B C_{Bm} + \sum_B C_{Be}^{(\varepsilon)} + \sum_B C'^{(\varepsilon^2)}_{Be} + \sum_B C_{Be}^{(\varepsilon^2)} \right)$$

Eq. 2.14

$$-\frac{F}{N_l k_B T} = \left(s_{MF} + \sum_B C_{Bm} + \sum_B C_{Be}^{(\varepsilon)} + \sum_B C'^{(\varepsilon^2)}_{Be} + \sum_B C_{Be}^{(\varepsilon^2)} \right)$$

Eq. 2.15

Like the FH, the LCT only needs three parameters to describe properties of a component. These are the lattice side length σ and the interaction parameters ε_1 and ε_2. By using only one set of parameters, the LCT can model all the isomers of a component. Up to now, the LCT considerers a maximum of four bonds or two bonds and two interactions. This results in a maximal order of $\varepsilon^2 z^{-2}$ for the theory. The LCT can model large polymers molecules up to a high degree of accuracy. However, it fails significantly in the range of the much shorter alkanes such as hexane. According to Zimmermann et al. (6), the extension of $\varepsilon^2 z^{-2}$ to $\varepsilon^2 z^{-3}$ improves the model noticeable for those cases. This is achieved by including contributions with z^{-3}, which only appear in contracted diagrams from the four bound cluster diagrams onwards. More specifically, the contracted $R_{4.4}$ and $R_{4.6}$ according to Brahznik (13) are included. A planned extension of the model to $\varepsilon^3 z^{-3}$ would require the inclusion of diagrams with up to six bonds and up to three interaction bonds.

3 Methodology

3.1 Additional Diagrams

The Lattice Cluster Theory (LCT) corrects the Flory Huggins Theory (FH), which it takes as mean field, with the help of cluster diagrams. Therefore, as shown in Eq. 2.15, the configural part of the FH s^{MF} is corrected by addition of the diagram contributions. These diagrams contain the substructures which can be found on the molecules and the interaction forces between adjacent segments. As the number of bonds in a diagram increases, its contribution decreases significantly. Freed (1) stopped the development of the diagrams at a maximum contribution of $\varepsilon^2 z^{-2}$. He included 17 entropic diagrams and 82 energetic diagrams in his model. These have up to four bonds, or up to two bonds and two interactions between the segments. The so selected upper limit of B=4 allows only two interactions, which in turn leads to a maximum exponent for the interaction parameter ε of two. The limitation of the exponent for the coordination number z results from the contribution of the diagrams. Here all parts of the contributions are omitted that contain a z to a power smaller than minus two. In this thesis only the influence of the entropic diagrams is considered. All possible entropic diagrams with up to four bonds are shown in Figure 2. The circles are the vertices and represent a segment. The connecting lines are the edges and represent the chemical bond between the segments. The energetic contribution is represented by the Mean field energy expression from the FH. This is discussed in more detail in chapter 3.4. Zimmermann (6) increased the allowed exponent for the coordination number z to minus three. The contributions with z^{-3} are considered but no new diagrams are included. According to Brahznik (13), who used graph theory to calculate the contributions of the contracted diagrams, diagrams with at least five bonds have only contributions with z^{-3} or smaller. It thereby allows the extension of the model to an order of $\varepsilon^3 z^{-3}$. To obtain symmetry, the diagrams with up to six bonds must be considered. Otherwise some of the higher diagram contributions will not cancel out each other and unphysical behaviour occurs. For the development of the model all entropic diagrams with up to six bonds must be determined. The entropic diagrams can be divided into three categories. These three have different properties and behave differently while calculating their contributions. The first category contains diagrams which consist of a single structure. Diagrams of the second kind consist of two

or more structures that are not connected directly. Diagrams of the third kind also consist of at least two not directly connected structures, of which at least two are on the same chain. All possible entropic diagrams can be classified into one of the categories.
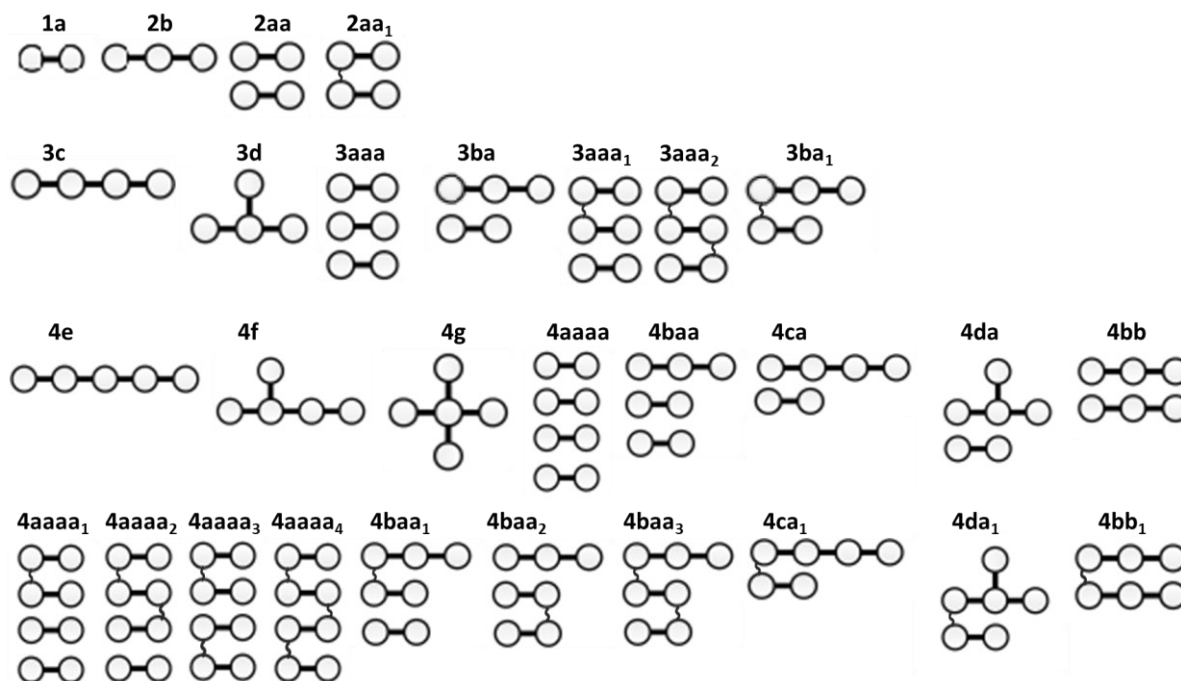
Figure 2: All entropic cluster diagrams with up to four bonds

Diagrams of the first kind consist of only one structure. For the diagrams with up to four bonds from Figure 2 this corresponds to {1a, 2b, 3c, 3d, 4e, 4f, 4g}. In the entropic diagrams, the edges correspond only to chemical bonds. They therefore follow the rules of organic chemistry, more precisely the rules of the alkanes. One vertex can be connected with a maximum of 4 other vertices. Edges may only exist between two adjacent vertices, a further distance would not allow a covalent bond. Structures with two bonds between the diagrams or circular diagrams are not considered since such cases are counted as monomers and are accounted by the parameters of the model. The segments can be rotated freely over the edges. This has been considered in the representation by always showing the longest chain and always starting to place branches on the left side. This corresponds to the rules of the standard nomenclature according to IUPAC (14). Since the structures follow the rules of the alkanes there is a corresponding structure for each isomer. This means that there are exactly as many diagrams of the first kind with five and six bonds as there are isomers for hexane and heptane. The number of possible isomers is a much-researched

field of organic chemistry. Bytautas and Klein (9) listed them with the help of chemical combinatorics. They started from alkyl radicals and applied the method of rooted trees, following the valid alkane rules, to arrive at the number of possible isomers. There are five isomers for hexane and nine for heptane. So, there are five diagrams of the first kind with five bonds {5h, 5i, 5j, 5k, 5l} and nine with six bonds {6m, 6n, 6o, 6p, 6q, 6r, 6s, 6t, 6u}. In total there are 21 diagrams of the first kind. These are listed in Figure 3.
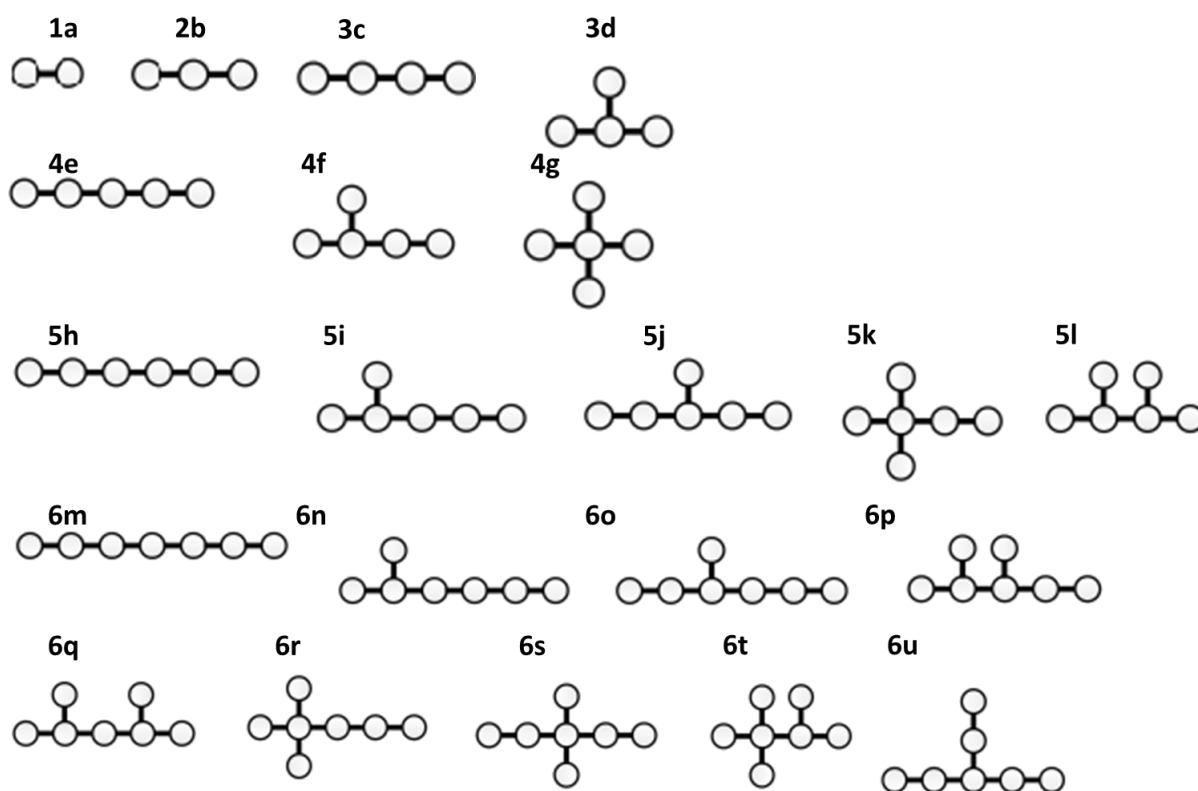
Figure 3:All inspected entropic cluster diagrams of the first kind

Diagrams of the second kind consist of more than one structure. These structures must not share any vertices. There is always at least one unoccupied bond between the individual structures when placing them on the molecule. These diagrams result from combinations of smaller diagrams of the first kind. In Figure 2 this corresponds to the eight diagrams {2aa, 3ba, 3aaa, 4ca, 4bb, 4baa, 4aaaa, 4da}. First, all possible diagrams with five bonds have been determined and then those with six bonds. The same counting method is used for both. The diagrams of the first kind with one bond less are used as a starting point. These are then combined with a diagram whose structures have fewer or the same number of bonds as the initial diagram. Diagrams of the third kind are left out, since a combination of any diagram with a diagram of the

third kind always results in a diagram of the third kind. The process is always started with the largest possible diagram to avoid double counting. Diagrams with four bonds can only be combined with diagram 1a to get five bonds, this results in three new diagrams {5ea, 5fa, 5ga}. Diagrams with three bonds require two bonds to get five bonds. They can therefore be combined with diagrams 2b and 2aa. This creates four new diagrams {5cb, 5caa, 5db, 5daa}. The diagram 2b with two bonds is combined with the diagrams 3aaa and 3ba, resulting in two new diagrams {5baaa, 5bba}. The last diagram 1a can only be combined with the diagrams 4aaaa, which creates one more diagram {5aaaaa}. So, there are ten new diagrams of the second kind with five bonds. With six bonds the same counting process is performed, starting with the diagrams with five bonds. One gets 22 diagrams of the second kind with six bonds {6ha, 6ia, 6ja, 6ka, 6la, 6eb, 6eaa, 6fb, 6faa, 6gb, 6gaa, 6cc, 6cd, 6caaa, 6cba, 6dd, 6daaa, 6dba, 6bbb, 6bbaa, 6baaaa, 6aaaaaa}. This results in a total of 40 diagrams of the second kind, which are listed in Figure 4.

Diagrams of the third kind consist of several structures like diagrams of the second kind. They result from the method used to calculate the combinatorial contribution of second kind diagrams. To prevent two structures of these diagrams from sharing a segment, the individual structures are always placed on different molecules. Third kind diagrams now cover the case where two or more structures are placed on the same molecule. If two structures are on the same molecule, this is represented by a wiggling line between the structures. In Figure 2 there are thirteen diagrams {aa1, ba1, ca1, da1, bb1, aaa1, aaa2, baa1, baa2, baa3, aaaa1, aaaa2, aaaa3}. So, they are closely related to the diagrams of the second kind. For each of these diagrams there is at least one diagram of a third kind. But since there can be more than one, the number of diagrams of this kind is considerably higher. The starting point is always a second kind diagram and from this the third kind diagrams are developed. Thus, one obtains 22 diagrams of the third kind with five bonds and 79 diagrams with six bonds. This kind of diagrams accounts for the largest share of the diagrams and therefore most of the time to calculate the diagram contributions. To avoid this, the method for calculating the combinatorial contribution of second kind diagrams has been modified instead. Nemirovsky (15) introduced a new method for this. The structures can be on the same molecule, but the possibilities of complete overlapping are counted. Furthermore, all diagrams that can be formed are subtracted from these.

With this method the third kind of diagrams become obsolete and can be omitted. This is discussed in more detail in chapter 3.3.
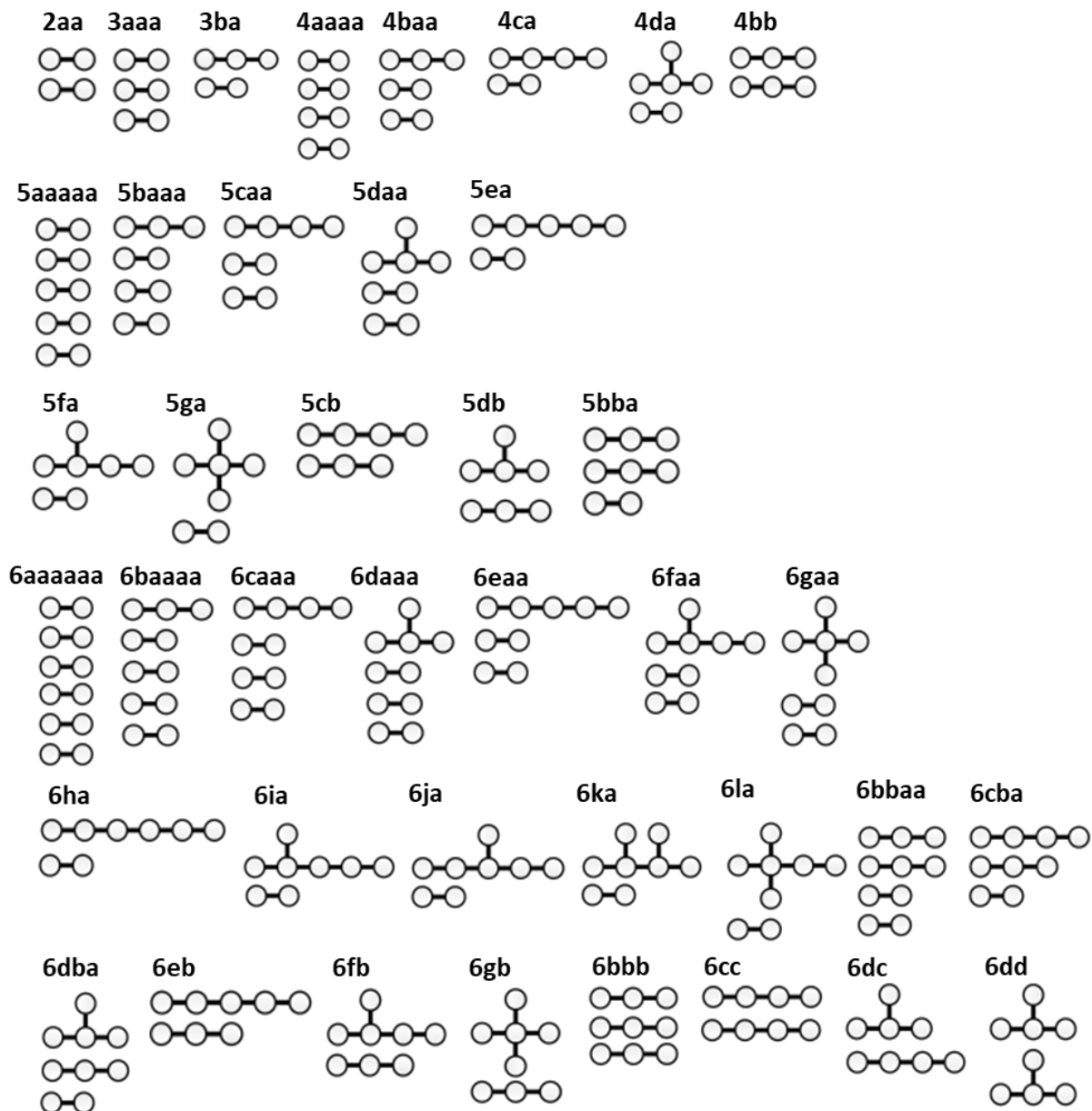
Figure 4:All inspected entropic cluster diagrams of the second kind

Each of the diagrams consists of cumulants. These cumulants are derived from Taylor series expansion of the logarithm of the sum of the cluster diagrams shown in eq. 2.7. The result of this series expansion is expanded and the terms with identical structures are cumulated. Each of these composite terms is a cumulant of the diagram. One can divide the resulting cumulants into two categories. First, there are the main cumulants that consist of only one cluster diagram. These come from the linear term of series development. Since diagrams of the first kind have only one structure,

they can also have only one cumulant. The second category, the sub-cumulants, is derived from the subsequent terms of series development. Each of these cumulants represents a product of several cluster diagrams. Each diagram of the second kind has at least one of these sub-cumulants. However, since these represent a product of two cluster diagrams, their contribution is negligible if the contribution of one of the diagrams is negligible. Therefore, all cumulants that have an unit made up of a single diagram 1a in are omitted. In particular, this reduces the number of cumulants in diagrams with many a structures. It further reduces the highest order of the Taylor series terms to the cubic terms. Thus, although most of the second kind of diagrams still have cumulants, the number of cumulants is significantly reduced.

By extending the upper limit of bonds in diagrams from B=4 to B=6, the way for extending the model to an order from $\varepsilon^3 z^{-3}$ was made possible. It leads to the introduction of a total of 46 new diagrams, 14 diagrams of the first kind and 32 diagrams of the second kind. By changing the methodology for determining the combinatorial part, the third kind of diagrams is omitted. This gives a total of 61 included entropic diagrams. In addition, the premature deletion of non-contributory cumulants further reduces the computational effort per diagram.

3.2   Contracting the Diagrams

The lattice-dependent part of a diagram contribution indicates how many postures a diagram can have. It depends only on the examined diagram and the selected lattice and is independent of the examined molecule. It can be represented as Eq. 3.1. Whereby the denominator α indicates the number of possibilities to find the segments of the diagrams in a lattice with N_l lattice positions. It includes the volume contraction but does not take into account the condition that two segments must be next to each other. For diagrams with up to four bonds, the first two terms of the expanded form of α are sufficient for performing the necessary polynomial division. Since all other terms only influence parts that approach zero in the thermodynamic limit. For diagrams with up to six bonds, however, the third term can still have an influence. The function Eq. 3.2 for the calculation of α can thus be displayed with the function Eq. 3.3 without the necessary information being lost. N_v is the number of vertices in the clus-

ter diagram. The two factors f_1 and f_2 stem from the Binomial coefficient of the product and are a function of N_v.

$$D_B = \frac{d_B}{\alpha}$$

Eq. 3.1

$$\alpha = N_l * (N_l - 1) * (N_l - 2) * \dots * (N_l - N_v + 1)$$

Eq. 3.2

$$\alpha \cong N_l^{N_v} * \left(1 - \frac{f_1}{N_l} + \frac{f_2}{N_l}\right)$$

Eq. 3.3

Since some cumulants are made up of more than one diagram, their α is the product of the α terms from the diagrams they are made up. The factor d_B stands for the number of permissible positions that the diagram can assume in the lattice. It can be calculated as the sum of the first Brilllouin zone of the limited sum of vertices of possible monomer positions, the product of the binding contributions.

$$\sum_{q_1,\dots,q_m \neq 0}^{1^{st} Brillouin\ zone} \sum_{i_1 \neq \dots \neq i_m} \prod_{\delta=0}^{m} b_\delta$$

Eq. 3.4

The restricted part of this sum makes solving it very complex. However, this restricted sum can also be represented by several unrestricted sums. More precisely, by subtracting all invalid sums from the unrestricted sum of the vertices over the possible monomer positions.

$$\sum_{i_1 \neq \cdots \neq i_m} = \sum_{i_1, i_2, \dots, i_m}$$

$$- \sum_{i_1, i_2, \dots, i_m} \delta\left(r_{i_1}, r_{i_2}\right) + \delta\left(r_{i_1}, r_{i_3}\right) + \cdots + \delta\left(r_{i_{m-1}}, r_{i_m}\right)$$

$$+ \sum_{i_1, i_2, \dots, i_m} \delta\left(r_{i_1}, r_{i_2}, r_{i_3}\right) + \cdots + \delta\left(r_{i_{m-2}}, r_{i_{m-1}}, r_{i_m}\right) + \cdots$$

$$+ \sum_{i_1, i_2, \dots, i_m} \delta\left(r_{i_1}, r_{i_2}, \dots, r_{i_m}\right) \qquad \text{Eq. 3.5}$$

An invalid posture can also be seen as an overlapping of two vertices. These vertices merge when overlapped. In graph theory, the merging of such vertices is called contracting and the resulting diagrams are called contracted diagrams (CD). This has been applied by Nemirovsky (15) to these invalid postures. As a result, the sums of invalid positions were displayed as CDs. The contribution of the CDs d_B derives from the sums in Eq. 3.5.

However, since the contribution are also tied to a diagram, Brazhnik (13) used graph theory to calculate and list all the necessary diagrams for the contributions. The original methodology is used as a starting point and is transformed in such a way that it only depends on the geometric properties of the diagram. The complex sum is reduced to a handy form Eq. 3.6. In this form $R_{B,m}$ is the value of one sum represented by a CD.

$$d_B = \sum_{m}^{N_v'} f_{B,m} * R_{B,m} \qquad \text{Eq. 3.6}$$

Not all formable CDs are necessary for the calculation of d$_B$. Many can be omitted for various reasons. These reasons can be recognized by four specific characteristics that the CD has.

- A vertex that is connected to itself by an edge

- A vertex that is connected to only one edge

- Two parts of a diagram that are only connected by a single edge

- A closed circle with an odd number of vertices
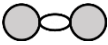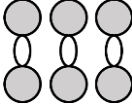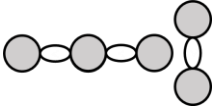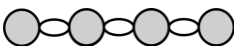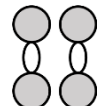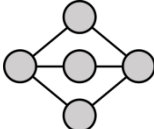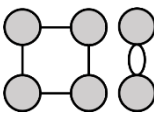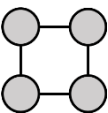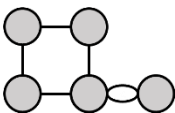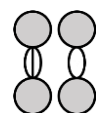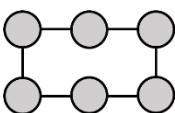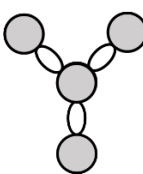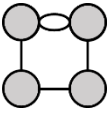
A vertex that is connected to itself by an edge is contradicted in the underlying delta function from function Eq. 2.3. Since the edge connects the same point twice, the value of the part $\delta(r_i, r_{i+1} + \alpha_\beta)$ is in the case of $i = i + 1$ always zero, because α_β is always nonzero.

A vertex that is connected to the rest of the diagram by only one edge and a part of diagram that is connected by only one edge disappear for the same reason. They do not satisfy the conservation of moment over every possible intersection. At least two intersections must occur to fulfil this condition.

Closed rings with an odd number of vertices are not possible in the case of a hypercube lattice. They therefore have no contribution. The number of vertices in a ring is equal to the number of bonds. In a hypercubic lattice, the edges can only go in the six directions of the cube faces. To form a circle from any chosen starting point, the circle must have for each bond a bond pointing in the opposite direction. The bonds only appear as pairs in the circles and must therefore have an even number. The case that a cluster diagram in a hypercube lattice forms an odd ring is therefore not possible.

According to Brazhnik (13), this omission reduces the number of CDs considered to only 26 CDs for diagrams with up to six bonds. Furthermore, the selected elimination criterion for contributions with a z exponent of less than z^{-3} means that nine additional CDs are not necessary. This shortens the contribution of some diagrams considerably. The 17 CDs under consideration are listed in Table 1 together with their contributions.

Table 1: Contracted diagrams used for the determination of the lattice dependent part with their contribution $R_{B,m}$

Contracted diagram	Structure	Contribution $R_{B,m}$	Contracted diagram	Structure	Contribution $R_{B,m}$
2.1		$\dfrac{N_l^3}{z}$	6.6		$\dfrac{N_l^9}{z^3}$
3.1		$\dfrac{N_l^4}{z^2}$	6.7		$\dfrac{N_l^8}{z^3}$
4.1		$\dfrac{N_l^5}{z^3}$	6.8		$\dfrac{N_l^7}{z^3}$
4.2		$\dfrac{N_l^6}{z^2}$	6.12		$\dfrac{N_l^7}{z^3}$
4.3		$\dfrac{N_l^5}{z^2}$	6.13		$\dfrac{3N_l^8}{z^3}$
4.4		$\dfrac{3N_l^5}{z^2} - \dfrac{3N_l^5}{z^3}$	6.14		$\dfrac{3N_l^7}{z^3}$
5.2		$\dfrac{N_l^7}{z^3}$	6.15		$\dfrac{15N_l^7}{z^3}$
5.3		$\dfrac{N_l^6}{z^3}$	6.16		$\dfrac{N_l^7}{z^3}$
5.4		$\dfrac{3N_l^6}{z^3}$			

A diagram can form a specific CD in several ways. By introducing the pre-factor $f_{B,m}$ for each CD, this is taken into account. This pre-factor is in the case of just two merged vertices Eq. 3.7.

$$f_{B,m}^{(d)} = - n_{B,m}$$

Eq. 3.7

Here the n_{Bm} stands for all different ways to form the contracted diagram from the original cluster diagram. In other words, how many distinguishable ways there are to merge two vertices. With this pre-factor some CDs count certain states multiple times. This error is corrected with some additional contraction diagrams. In these diagrams, further vertices are merged. It continues until the point where all vertices merge and all bonds form loops. This means that CDs change their sign depending on the number of merged vertices. This change in the sign and the number of times a multiple contraction diagram is formed must again be included by the pre-factor f_{Bm}. This generalizes the factor to the form Eq. 3.8.

$$f_{B,m}^{(d)} = (-1)^{N_v - N_v'} * \sum_{\eta}^{a} n_{B,m,\eta} * \prod_{\lambda=1}^{N_v'} (k_\lambda - 1)!$$

Eq. 3.8

In this form N_v stands for the number of vertices in the cluster diagram and N_v' for the number of vertices in the CD. The difference between the two is equal to the number of merged vertices. In many cases a possible CD can be formed in several different ways. The variable a stands for all possible appearances of the CD. This can easily be illustrated by using the example of cluster diagram e to the CD 4.2. In Figure 5 it can easily be seen that either the fourth and the second vertex are merged or the first, third and fifth vertex. Both forms of appearance have the same number of vertices and have the same number of overlays but are distributed differently. While for appearance (1) there is a single vertex and two vertices overlaid once, for appearance (2) there are two single vertices and one vertex overlaid twice. The counter $n_{Bm,\eta}$ counts how many ways an appearance can be formed. One gives each vertex an identity and search for all the different combinations of vertices. In the example of

Figure 5 there is for each appearance only one unique combination. The following product goes over all vertices of the contracted diagram. Multiply the factorial of the variable k_λ minus one. k_λ is the number of superimposed vertices at that position. If you subtract one you get the number of merges at this position. Since these can take place in different orders, one takes the factorial to calculate the complete amount of necessary corrections.
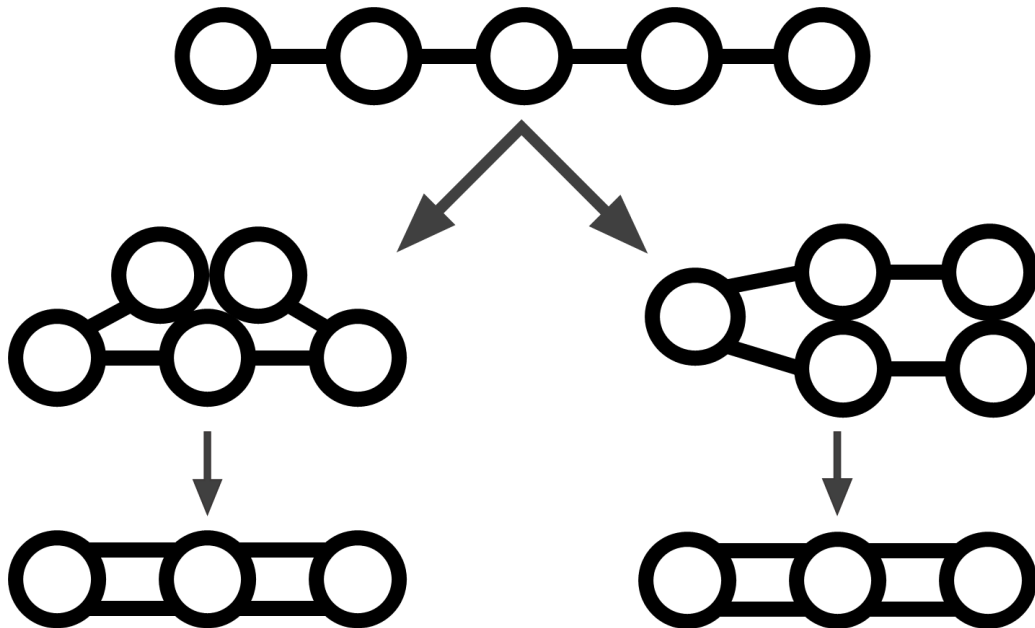
Figure 5: Both appearances of the CD 4.2 from the cluster diagram 4e

In the case of several cumulants, the contribution of the lattice dependent contribution is determined separately for each one.

With the determination of the pre-factor $f_{B,m}$, all variables previously unknown for the determination of the lattice-dependent contribution DB are now available. Starting from a cluster diagram, the following procedure is performed.

1. determination of the CDs which can be formed from the cluster diagram

2. determine the possible appearances and the number of possible ways of forming them

3. the calculation of the pre-factor $f_{B,m}$

4. determine d_B by adding up the products of the pre-factors $f_{B,m}$ and the contribution $R_{B,m}$ of the CDs

5. polynomial division of the contribution d_B by the first three terms of the expanded form of α

The procedure contains mostly analytical formulas and is therefore simpler to tackle with. However, the first two steps are somewhat complex. The first step is done by manually checking all valid CDs with the same number of bonds. The second step can also be counted relatively easily for diagrams with up to four bindings. For diagrams with up to six bindings, however, this becomes significantly more complex. The number of appearances increases significantly and must be counted in accordance with certain rules. However, the number of the respective arrangement of the vertices in such an appearance is still significantly higher. These arrangements can no longer be determined with reasonable effort. Instead, the methods of combinatorics are employed.

At the first step of the procedure it is possible to discard some of the valid CDs in advance. In the diagrams of the first kind it is not possible to create CDs consisting of several structures. During contracting, a structure can only be joined together, but not split apart. It is therefore limited to CDs consisting of one structure. The largest formable ring of a diagram depends on the longest chain that can be found in the diagram. CDs with larger rings than the chains are not formable. In the case of diagrams of the second kind, CDs consisting of several structures can be formed, but the structures of the individual sub CDs must not have fewer bonds than the structures of the CD. For both kinds, the maximum number of edges connected to a vertex can only increase and not decrease. CDs where this number is less than that of the cluster diagram are also not able to form.

The original cluster diagram is used to determine the appearances which can be formed. The vertices are assigned numbers starting from one vertex. It is important to note that even numbers are only connected with odd numbers and vice versa. For this purpose, it is possible to omit individual numbers from the numbering. If an odd ring is created while contracting a diagram, it cannot be removed by contracting. It can only be split up into two smaller rings, one of which must be odd. All CDs that can be made from it are non-contributory. Between two vertices associated with an even number or two associated with an odd number there is always an even number of edges. If one only merges even with even and odd with odd vertices, only even rings can be formed during contracting. The possible formation of odd rings can be avoided. In case the diagram is of the second kind and has several structures, this rule only applies within one structure. By merging the vertices of two structures they

become one single structure and the rule becomes valid again. As with step 1, the selection of CDs that can be formed, the number of bonds tied to a vertex cannot be reduced. Vertices of the original diagram can only occupy a position in the CD if at least as many edges are attached to them as in the original diagram. These rules limit the number of appearances to be checked. Nevertheless, all possible ways of forming the appearances must be examined.

However, the number of arrangements of vertices in an appearance can be solved with the help of combinatorics. To do this, first some properties of the CDs, the appearance and the cluster diagrams must be determined. The number of arrangements that a diagram occupies in an appearance can be calculated with Eq. 3.9.

$$n_{B,m,\eta} = \frac{n_p * n_o}{n_{pos} * s} \qquad\qquad \textbf{Eq. 3.9}$$

In the numerator there are the variables n_p and n_o, the first represents the number of states the structures can take and the second the number of sequences in which the similar structures can be placed. The denominator contains the properties of the appearance itself. n_{pos} depends on the number of equivalent positions in the diagram and the factor s indicates that some appearances are symmetrical over some axes.

For the determinations, the first step is to identify the number of possible states n_p. This indicates the number of ways in which the structures can be positioned in their intended position in the appearance. They thus depend on the structure under consideration and on the position. The product of the possible states over all positions in the diagram illustrates this mathematically. The number of positions is equal to the number of structures in the diagram because each position must be occupied. While structure a, with only a single edge between two vertices, always has two states, with structure b, having three vertices and two edges, it already depends on its position in the appearance. Structure b can either have two states if it occupies three vertices in a position and is straight or a single state if it occupies only two vertices and is folded. Of the diagrams under consideration, except for structure o, each structure can take several states in at least one position. This is because all other diagrams have at least one symmetry axis.

$$n_p = \prod_i^{positions} n_{p,i} \qquad \text{Eq. 3.10}$$

If the diagram has several identical structures, these structures can occupy one position. To include such a case, n_o is introduced. Since diagrams of the first kind always consist of only one structure, this factor is always one in these cases. It becomes important for diagrams of the second kind. Here one can assume that the positions of the appearance are filled with the structures one after the other. In order to observe all sequences of filling, the product of the factorial is taken from the number of identical structures $n_{s,j}$. This product depends only on the type and number of structures in the cluster diagram and is therefore independent of the form of appearance and the CD.

$$n_o = \prod_j^{type\ of\ structures} n_{s,j}! \qquad \text{Eq. 3.11}$$

The number of equivalent positions n_{pos} in the denominator is again a function of appearance. If two positions are identical, they do not bring a new arrangement, but they are still counted twice. Identical means in this case that they share all their vertices with the same structures. To counteract this, the number of arrangements is halved in that case. If one continues to follow that thought, it can occur on some CDs that three structures are completely identical. In this case, it is shown that the same arrangement is counted six times. This is because the variable n_o considers all possible arrangements of the structures in one position. It is necessary to divide by the factorial of the number of equal positions. In the case that several groups of such identical positions exist, the faculties resulting from them are multiplied with each other. This also occurs if different types of structures have identical positions. If the structures of the publication form itself are identical, the faculty of the number of identical structures must be multiplied again. Two structures are identical if the freestanding structures are made of the same type of structures and the vertices are merged in

the same way. The variable n_{pos} is thus mathematically describable as the product of the products of the individual identical positions and the product of the identical CD structures.

$$n_{pos} = \overset{CD\ structures}{\underset{l}{\prod}} n_{str,l}! * \overset{CD\ positions}{\underset{k}{\prod}} n_{pos,k}!$$

Eq. 3.12

The variable s stands for the symmetries which can be found in the appearance. These are determined individually and then multiplied in the same way as the number of equivalent positions. Symmetry means that a structure of an appearance can be rotated around an axis of symmetry without changing the arrangement of the positions. In most cases two indistinguishable states can result from the rotation. The only exception to this is the CD 6.12, which creates six different indistinguishable states when the arms are rotated and thus interchanged. s can easily be represented as the product of these states.

$$s = \overset{symmetry\ axis}{\underset{ax}{\prod}} s_{ax}$$

Eq. 3.13

By inserting the four expressions into the equation (Eq. 3.9), one obtains a rather complex formula for calculating the possible arrangements of the vertices. Instead of listing all possible arrangements, it is now sufficient to use equation (Eq. 3.14) for each form of appearance.

$$n_{B,m,\eta} = \frac{\prod_i^{pos} n_{p,i} * \prod_j^{struc} n_{s,j}!}{\prod_l^{CD\ struc} n_{str,l}! * \prod_k^{CD\ pos} n_{pos,k}! * \prod_a^{axis} s_a}$$

Eq. 3.14

In the case of cumulants, they are a product of several diagrams and cannot interact with each other. They can form a common CD but are not allowed to share a vertex.

This is because the contributions of the composite CD are only the product of the CDs they are composed of. To determine the possible forms of appearance of these CDs, all diagrams should be kept separate. While n_p and s are to be treated equally by all cumulants, this changes for n_o and n_{pos}. For n_o, only the structures of the same type may be selected, which are also in the same diagram of the cumulant. The same structures that are in different diagrams are treated in the same way as different structures. For n_{pos}, identical positions of the CD that are assigned to different diagrams of the cumulant are not considered identical. They are regarded as different positions. Within a diagram of the cumulant, identical positions are still regarded as identical.

By using the number of arrangements of the respective appearances one can now calculate the contribution of each cluster diagram using equation Eq. 3.8, Eq. 3.6 and Eq. 3.1. The polynomial division of Eq. 3.1 results in terms with a decreasing order of the number of lattice locations N_l. Terms whose order is less than $-(n-1)$ would disappear in the thermodynamic limit after multiplication with the combinatorial contribution. n is in this case the number of structures in the diagram.

3.2.1   Example 5daa

Diagram 5aad is used to illustrate this procedure presented on page 23. The diagram has two cumulants, whose contribution cannot be omitted. Both are shown in Figure 6. The one the left is the main cumulant $5daa_1$ and the one on the right side is the cumulant $5d|aa_2$. The first step of the procedure is the determination of the formable contracted diagrams. For the cumulant $5daa_1$ these are all CDs determined by Brazhnik (13) which have a valid contribution and five bonds. With the second cumulant $5d|aa_2$ it is only CD 5.2 formable.

The second step in the procedure is the determination of the possible appearances. For each formable CD, the possible appearances are listed in Table 2.

The third step is now the calculation of the pre-factors with the help of these appearances. Since n_o is only dependent on the cluster diagram, it is the same for all appearances. It consists of three structures of which two are identical, these have two possibilities to be distributed in the appearances. The number of distribution possibilities n_o is therefore two.

$$5daa_1 \qquad\qquad 5d|aa_2$$
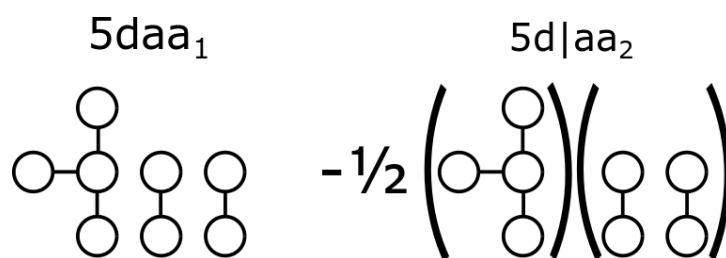
Figure 6: Cumulants of the diagram 5daa and their pre-factor

Table 2: All formable appearances from the cumulants of diagram 5daa

CD for 5daa₁	Appearances of the CD
5.2	
5.3	
5.4	
CD for 5d|aa₂	
5.2	

The CD 5.1 has no contribution with an z exponent of minus three or higher. Its pre-factor is therefore obsolete.

For CD 5.2 there is only one appearance. The structure a can take two states. For the structure d there is only one possible state. The two positions for structure a are identical which leads to a n_{pos} of two. The second structure of the CD which consists of two knots and two bindings can be rotated around an axis without changing the

arrangement of the positions. It therefore has an s of two. By inserting it into equation Eq. 3.14 this results in two possible arrangements for the appearance. The difference of the vertices is even, which means that the pre-factor is positive. The CD has four vertices two with two merged vertices, one with three merged vertices and one with a single vertex. The resulting pre-factor is Eq. 3.15.

$$f_{B,m} = (-1)^{8-4} * \left(2 * ((\ 1-1)! * (2-1)!^2 * (3-1)!)\right) = 4 \qquad \text{Eq. 3.15}$$

For the CD 5.3, there are four appearances. The first two appearances differ only in the position of the structure d. For both positions of the structure n_p and n_{pos} are identical. At the same time, both forms of appearance have no symmetry s, it is therefore one. The number of arrangements is therefore the same for both. They both have two states for each structure a and the two positions are identical. They can therefore be arranged in four different ways. The third type has three possible states for structure d and two for structure a. The positions of the individual structures are not identical and result in $n_{pos} = 1$. The number of arrangements for the third appearance is therefore 24 possible arrangements. The fourth appearance has three states for the structure d and two for the a's. It also has no symmetry. However, the positions of the structures a are identical, which results in a n_{pos} of 2. The fourth form of appearance therefore has twelve possible arrangements. With the number of arrangements and merged vertices per appearance the pre-factor of the CD can be calculated. Since the difference in the number of vertices in this CD with five is odd, the pre-factor is negative as seen in Eq. 3.16.

$$f_{B,m} = (-1)^{8-3} * \left(\begin{array}{c} 4 * ((\ 2-1)! * (3-1)! * (5-1)!) \\ + 4 * ((\ 2-1)! * (3-1)!^2) \\ + 24 * ((\ 2-1)! * (3-1)!^2) \\ +12 * ((\ 2-1)! * (3-1)!^2) \end{array} \right) = -256$$

<div align="right">Eq. 3.16</div>

The CD 5.4 has again only one possible appearance. In this form the structure d can take three states and the structure a, two states. None of the positions is identical and it has no symmetry. Both variables in the denominator are therefore one. The resulting pre-factor is therefore Eq. 3.17.

$$f_{B,m} = (-1)^{8-4} * \left(24 * \left((\ 1-1)! * (2-1)!^2 * (3-1)!\right)\right) = 48 \qquad \textbf{Eq. 3.17}$$

The cumulant $5aa|d_2$ can only form the CD 5.2 This has only one valid appearance form. The first part of the cumulant consists of two structures a, and these can each take up two states. However, the positions are identical and have symmetry. The second part consists only of the structure d, which can only take up one state and again has no symmetry. The number of arrangements is therefore two and the pre-factor is therefore the same as in Eq. 3.15.

With the pre-factors and the contributions of the CDs listed in Table 1 the contribution d_B can now be calculated for both cumulants. In the fourth step this is done by multiplying the contributions with the correlating pre-factor and summing them up. It is shown in Eq. 3.18 for the cumulant $5daa_1$ and in Eq. 3.21 for $5d|aa_2$.

$$d_{5daa_1} = 4 * \frac{N_l^7}{z^3} - 256 * \frac{N_l^6}{z^3} + 48 * \frac{3 * N_l^6}{z^3} \qquad \textbf{Eq. 3.18}$$

$$d_{5d|aa_2} = 4 * \frac{N_l^7}{z^3} \qquad \textbf{Eq. 3.19}$$

The fifth step is to divide this sum by α. The first cumulant has a total of eight vertices. These result in an α of Eq. 3.20. If you expand this form you get the form which consists of eight terms. Of these, only the three with the highest N_l orders are important for the calculation of the diagram contributions. The remaining terms influence only parts of the contribution which are approaching zero in the thermodynamic limit. α can therefore easily be approximated with Eq. 3.21.

$$\alpha_{5daa_1} = N_l * (N_l - 1) * \ldots * (N_l - 7) = N_l^8 - 28 * N_l^7 + 320 * N_l^6 + \cdots \qquad \text{Eq. 3.20}$$

$$\alpha_{5daa_1} \cong N_l^8 * \left(1 - \frac{28}{N_l} + \frac{320}{N_l^2}\right) \qquad \text{Eq. 3.21}$$

In the second cumulant both parts consist of four vertices. α results from the product of the two parts. It thus results from the equation Eq. 3.22. As with the first cumulant, it can be expanded and approximated by Eq. 3.23.

$$\alpha_{5d|aa_2} = (N_l * (N_l - 1) * \ldots * (N_l - 3)) * (N_l * (N_l - 1) * \ldots * (N_l - 3))$$

$$= N_l^8 - 12 * N_l^7 + 58 * N_l^6 + \cdots \qquad \text{Eq. 3.22}$$

$$\alpha_{5d|aa_2} \cong N_l^8 * \left(1 - \frac{12}{N_l} + \frac{58}{N_l^2}\right) \qquad \text{Eq. 3.23}$$

The lattice dependent fraction of the two cumulants can now be calculated with α and d_B. The polynomial division required for this can already be aborted after the second term. The cluster diagram consists of only three structures, so the lattice-dependent contribution of the cumulants only needs to be developed up to N_l to order minus two. The second term of the first cumulant does not have a contribution. It thus results in the contributions Eq. 3.25 for the first cumulant $5daa_1$ and Eq. 3.27 for the second cumulant $5d|aa_2$.

$$D_{6daa_1} = \frac{4 * \dfrac{N_l^7}{z^3} - 256 * \dfrac{N_l^6}{z^3} + 48 * \dfrac{3 * N_l^6}{z^3}}{N_l^8 * \left(1 - \dfrac{28}{N_l} + \dfrac{320}{N_l^2}\right)} \qquad \text{Eq. 3.24}$$

$$D_{6daa_1} = \frac{4}{N_l * z^3} \qquad \text{Eq. 3.25}$$

$$D_{6d|aa_2} = \frac{4 * \frac{N_l^7}{z^3}}{N_l^8 * \left(1 - \frac{12}{N_l} + \frac{58}{N_l^2}\right)} \qquad \text{Eq. 3.26}$$

$$D_{6d|aa_2} = \frac{4}{N_l * z^3} + \frac{48}{N_l^2 * z^3} \qquad \text{Eq. 3.27}$$

3.3   Correction diagrams in the combinatorial part

The combinatorial part of the cluster diagrams stands for the number of possibilities to find the diagrams in the considered system. This part therefore depends on the considered diagram and the considered system of substances. It is independent of the underlying lattice and the possible posture of the individual diagrams. In the case of the first kind of diagrams, it can be determined by the sum Eq. 3.28 of the product of the frequency of the diagram N_i in one molecule of the component and the number of molecules n_μ of one component over all components of the system. This product indicates how often the structure is found in all molecules of a component.

$$\sum_{\mu}^{k} N_i * n_\mu \qquad \text{Eq. 3.28}$$

The number of molecules is the total number of molecules of this type in the system. The frequency of a diagram in a component represents how often the structure of the diagram can be found in the component. It counts how often the individual bonds in the component form the structure of a diagram. As soon as only two structures can be distinguished by a single bond, they are counted. The combinatorial part gives the diagram contribution the information about the system. Since diagrams of the second kind can consist of several structures, all possible combinations of their positions must be taken into account. For example, structures can be located on different molecules or even different components. The sum Eq. 3.28 for first kind diagrams changes into a multiple sum Eq. 3.29. In this case, the product of the number in all molecules of a component of both structures is summed up. The sum must be calculated

individually for each structure. So, for each new structure a sum for all components is added.

$$\sum_{\mu}^{k} \sum_{\lambda}^{k} N_{i,\mu} * n_{\mu} * N_{j,\lambda} * n_{\lambda}$$

Eq. 3.29

If a diagram has several structures of the same type, it can happen that the resulting positions are indistinguishable. They do not lead to a new state of the system but are still counted in all the possible combinations. The product must be divided by the factorial of the number of identical structures on the same component to correct for this counting error. In cases where this occurs with several components or structures, the product of the factorials is taken. It is inserted in the multiple sum of Eq. 3.30 as f_{eq}.

$$\sum_{\mu}^{k} \sum_{\lambda}^{k} f_{eq} * N_{i,\mu} * n_{\mu} * N_{j,\lambda} * n_{\lambda}$$

Eq. 3.30

Two structures must not share a vertex. In this case they are not separated on the molecule but represent a different diagram. To avoid this Freed (1) uses the approach that two structures of a diagram are never located on the same molecule. This is mathematically converted into the sum of Eq. 3.30 by reducing the number of molecules with each following structure by one. Diagrams that are on different components cannot be on the same molecule. Therefore, the number of molecules only has to be reduced if the counting indexes of the sum are equal.

$$\sum_{\mu}^{k} \sum_{\lambda}^{k} f_{eq} * N_{i,\mu} * n_{\mu} * N_{j,\lambda} * (n_{\lambda} - \delta(\mu, \lambda))$$

Eq. 3.31

The omission of several structures on a chain requires that they are integrated in a different way. Therefore, diagrams of a third kind were introduced. These diagrams

contain at least two structures on the same molecule. If they do, there is a wiggly line drawn between the structures to symbolize this. For each case, the combinatorial part left out for diagrams of the second kind, there is a diagram of the third kind. This means that every possible combination of several structures is necessary. If two combinations are indistinguishable, they may only be counted once. The number of diagrams of the third kind is significantly higher than the number of the second kind. Which means that these diagrams take up the majority of all diagrams. When including diagrams with up to six bonds 178 diagrams are taken into account. 117 of these diagrams are diagrams of the third kind, which is 65 percent of the diagrams. Each diagram contains a combinatorial and a lattice-dependent portion. Diagrams of the third kind thus make up the majority of the work required to extend the model. Omitting the third kind of diagrams would reduce the amount of work involved in extending the model.

Nemirovsky (15) introduced a new method of calculating the combinatorial part of the diagram contributions for diagrams of the second kind. This method allows individual structures of the diagram to be placed on the same molecule. This makes third kind diagrams obsolete, because the contributions of these diagrams are now also included in second kind diagrams. By allowing more than one structure on a molecule chain, the combinatorial part for second kind diagrams would change back to the form Eq. 3.30. This form, however, allows the overlapping of the vertices. This overlapping can only occur if there are several structures on one molecule. If they are on other components, the number of positions is simply multiplied. A distinction is made between two cases, either one structure completely covers another structure, or the structures only share some vertices.

For one structure to completely cover another structure, both must be on the same molecule and one structure must be able to completely cover the other. One structure is able to completely cover another if they are the same structure or the covered structure can be identified in the other. Two different structures that have the same number of bonds can therefore not completely overlap. If a structure is completely covered, it cannot occupy one or more positions in the system. The number of missing positions depends on how often the structure can be identified in the other one and is called $N_{i,j}$. This can easily be described mathematically by the sum Eq. 3.32. The first placed structure can occupy any position within a component. Its number of

possible positions is still the product of the frequency of the diagram N_i in one molecule of the component and the number of molecules n_μ of that component. When adding the possible positions of the next coverable structure, the omitted positions $N_{i,j}$ are subtracted from this number. The number becomes a polynomial term. With each further addition, all positions of the previous placed structures must be considered. However, since the previous structures can still partially overlap, the smallest diagram that can be created by partially overlapping these structures is formed and checks how many positions are omitted by these structures. So, the number of positions $N_{i,j}$ is subtracted from the placed diagram.

$$\sum_\mu^k \sum_\lambda^k f_{eq} * N_{i,\mu} * n_\mu * (N_{j,\lambda} * n_\lambda - N_{i,j} * \delta(\mu,\lambda))$$

<div align="right">**Eq. 3.32**</div>

Since the polynomials depend on the sequence of the placement, the sequence is important. The sequence of the polynomials can no longer be freely chosen. Instead, you have to make sure that the first placed structures cannot be covered by any of the other structures. Then the next structures are placed in a way that they can only be covered by the previous structures. A structure placed later must either not be able to cover the previous ones or be the same structure as the previous one. The number of omitted positions increases with each new polynomial.

The structures a and b can be found in any structure with more bonds. They can therefore be covered by any larger structure. At least one of the two structures are also present in all, but three cluster diagrams considered. However, two of these diagrams {6cc, 6dd} consist of the same structures and can form a complete overlap. The only cluster diagram that does not have complete overlap is therefore the diagram 6cd.

With this diagram, partial overlapping of several bonds can still occur. In this case, however, they only share some vertices. If these cases were also handled as omitted positions, the number would depend on the respective position. Depending on where the structure is located in the system, a vertex can then prevent one, several or no position at all. The number would therefore be different for each position. According to Nemirovsky (15), these partial overlaps are allowed instead. The resulting error

includes the combinatorial part of another diagram in a diagram. Namely of any diagram that can be created by partial overlapping of two structures. The number of incorrectly counted positions can therefore be represented by the number of these diagrams. By subtracting these combinatorial parts from the Eq. 3.32 one obtains the combinatorial part of the considered diagram. These correction diagrams (CorD) can often be formed in several different ways. Each different type is counted separately in the combinatorial contribution of the diagram. This means that each CorD requires a pre-factor f_{cd} which indicates how many ways the cluster diagram can form it. To determine the pre-factor f_{cd}, the number of ways to find the structures in the CorD can be counted. Only those arrangements can be counted where all vertices of the CorDs are occupied. In addition, indistinguishable arrangements may only be counted once since multiple counting has already been corrected by the factor f_{eq}. The possible orientations of the CorD in the lattice are not taken into account by the factor f_{cd}. This is completely considered by the CorD itself. The CorD itself can have several identical structures, just like the cluster diagrams. With these, multiple counting of identical arrangements must also be avoided. This also results in a separate f_{eq}. By subtracting the CorDs from the sum Eq. 3.32, the form Eq. 3.33 is obtained for the combinatorial part. To simplify the formula, the sums of the individual diagrams are expressed as $\gamma_{B,m,i}$.

$$\sum_{\mu}^{k} \sum_{\lambda}^{k} f_{eq} * N_{i,\mu} * n_{\mu} * (N_{j,\lambda} * n_{\lambda} - N_{i,j} * \delta(\mu,\lambda))$$

$$-f_{cd} * \sum_{\mu}^{k} f_{eq} * N_{CorD,\mu} * n_{\mu}$$

$$= \gamma_{B,m,i} - f_{cd} * \gamma_{B,m,CorD} \qquad \textbf{Eq. 3.33}$$

For diagrams with more than two structures, both types of overlapping can also occur in the CorDs. The omitted items from a complete overlap are to be handled in the same way as in the individual diagrams. The structures are placed in an orderly manner and the omitted structures are subtracted. For the partial overlapping of the structures, further CorDs are created which correct the original CorDs. These CorDs

are to be handled in the same way as the original CorDs. For easier distinction, however, they are called CorDs of second order. As long as a CorD has more than one structure, it can again overlap vertices and must therefore be corrected with further CorDs. So, there are as many orders of diagrams in the combinatorial part as there are structures in the cluster diagram.

CorDs can be formed from the structures of the actual cluster diagram and the structures of the lower-order CorDs. Their pre-factor f_{cd} is no longer dependent on a single diagram. It can be considered as the sum of the individual pre-factors $f_{cd,i}$ for the formation from the lower-order diagrams. Since the CorDs can already be formed in several ways from the cluster diagram, the pre-factor $f_{cd,i}$ must be multiplied by the respective pre-factors f_{cd}. The pre-factor for the original cluster diagram is one because it can only be formed by itself. The sign of the terms is changed with each order. To take this change into account, the sign is moved into f_{cd} Eq. 3.34 and the original subtraction becomes the sum Eq. 3.35.

$$f_{cd} = - \sum_{j}^{diagrams} f_{cd}^{(j)} * f_{cd,i}^{(j)}$$

Eq. 3.34

$$\gamma_{B,m} = \gamma_{B,m,i} + \sum_{j}^{CorD} f_{cd}^{(j)} * \gamma_{B,m,j}$$

Eq. 3.35

Cumulants that consist of more than one diagram are treated by the combined contribution as if their structures are on different components. Same structures on different components in different diagrams are distinguishable and are not corrected with pre-factor f_{eq}. They cannot overlap and do not influence each other, neither the number of omitted positions nor the possible CorDs. Since the CorDs do not share any vertices between the two diagrams, they are always composed of several non-interacting diagrams. It should be noted, however, that some CorDs are formed several times by different diagrams of the cumulant. They then must be counted several times.

In the thermodynamic limit, the contributions of some CorDs go towards zero. The number of molecules in system n_μ varies with the size of the investigated system. It would go approach infinity in the thermodynamic limit like N_l. The number can also be expressed by the volume fraction φ_i of the component in combinatorial part through Eq. 3.36.

$$n_\mu = \frac{\varphi_i * N_l}{M_i}$$

Eq. 3.36

n_μ equals the number of segments in the total lattice sites N_l multiplied by the volume fraction and divided by the number of segments per molecule M_i. Instead of several variables going towards infinity, only N_l goes towards infinity in this form. The order of the number of lattice sites N_l is equal to the number of structures in the diagram. When multiplying the combinatorial contribution by the lattice-dependent contribution, only a few terms remain whose lattice number N_l is not in the denominator and thus approaches zero. The less structures a CorD has, the more likely it is to be omitted. In order not to use CorDs whose contribution is approaching zero, the number of necessary structures can be calculated in advance. However, the lattice -dependent contribution must first be known. The maximum order of N_l in the denominator of the lattice-dependent contribution plus one corresponds to the minimum number of nec-essary structures. The additional one comes from the additional normalization of the free energy to make it independent from the system size.

For a convenient check whether the determined combinatorial part of the diagram is correct, the system under consideration can be simplified considerably. In a system where there is only one molecule, the possibilities to find the diagram in this molecule can be manually counted. In such a system Eq. 3.33 takes the form Eq. 3.37. Because there is only one molecule n_μ is equal to one and does not have to be replaced by Eq. 3.36. The sums over the single components are also omitted because there can be only one component each. An error due to the wrong counting of f_{eq} or the missing positions, with several components can therefore not be checked in such a system. But there is a good clue if the pre-factors f_{eq} and f_{cd} are correct in the case that all are

on one component. These can then be converted to the other cases relatively easily. Since the system consists of only one molecule, the application of the thermodynamic limit is not reasonable. In this system it would have no effect on n_μ and therefore on the total sum. The simplification of omitting some CorDs cannot be made here.

$$f_{eq} * N_{i,\mu} * (N_{j,\lambda} - N_{i,j}) - f_{cd} * f_{eq} * N_{cor,\mu} \qquad \text{Eq. 3.37}$$

To determine the combinatorial contribution of a diagram, the following steps have been performed:

1. check which correction diagrams can be formed based on the structures of the diagram.

2. determine the pre-factor f_{eq} for all diagrams

3. determine the pre-factor f_{cd} for all correction diagrams starting from the cluster diagram

4. determine the order of placement for all diagrams and the omitted positions for the individual structures

5. repeat the procedure for all cumulants

Step four varies slightly between possible combinations of components and must be performed separately for each combination. As a result, the individual terms of each sum change by the number of positions omitted. In the case of several identical structures, each possible combination of components is counted several times, which is cancelled out by the pre-factor f_{eq}.

3.3.1 Example 5bba

The diagram 5bba illustrates how the combinatorial part of a cluster diagram is determined. As with determining the lattice dependent fraction, the procedure is discussed step by step. The diagram 5bba consists of the structures a and b and can form two valid cumulants, the main cumulant $5bba_1$ and the cumulant $5b|ba_2$. By partially overlapping the vertices of the individual structures, the first cumulant can form 15 correction diagrams (CorD). Of the twelve diagrams, seven are first-order diagrams and five are second-order diagrams. The first order diagrams are {ca, da, ea, fa, ga, cb, db} and the second order diagrams are {e, f, g, h, i, j, k, l}.

After it is known which CorDs can be formed, the pre-factor f_{eq} can be determined for these and the cluster diagram itself. Only the cluster diagram itself has the same structure two times. Therefore, f_{eq} is for this ½ and for all other CorDs one. If one of the two b structures are placed on a different component, the two b structures are no longer interchangeable since multiple counting of the combination would cancel out the factor f_{eq}.

The calculation of the pre-factor f_{cd} is determined for each CorD based on the cluster diagram 5bba itself. For example, the diagram ca can be created if the two b structures each share two vertices. As shown in Figure 7, this can be done in only one way. The two b structures share the central bond of structure c. The resulting pre-factor f_{cd} is therefore minus one. This would also result from the equation Eq. 3.34.
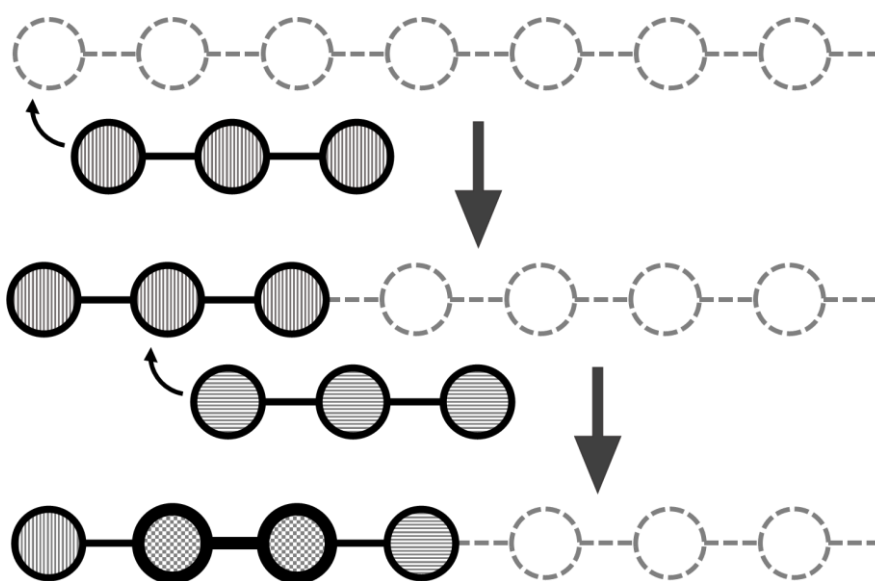
Figure 7: Overlaying of two b Structures to create a c Structure

In this case, the structure a can be placed freely from the other diagrams and thus lead to overlapping of individual vertices. In Table 3 the pre-factors for the first order CorDs are listed.

Table 3: The pre-factors for the correction diagrams of the first order for the cumulant $5aab_1$

Correction diagram	Pre-factor f_{cd}	Correction diagram	Pre-factor f_{cd}	Correction diagram	Pre-factor f_{cd}
ca	-1	fa	-1	db	-3
da	-3	ga	-3		
ea	-1	cb	-2		

It is noticeable that all first order diagrams always have one structure less than diagram 5bba. This is not always the case. For example, with the diagram 6bbb, diagram 3d can only be formed from the initial diagram and is therefore a first-order diagram. The second order CorDs can be formed from the initial diagram and from at least one of the second order diagrams. Thus, diagram 4e can be formed from 5bba but also from 4ca and 5cb. These can each form it in two different ways, as shown in Figure 8. Table 4 shows the pre-factor for each of the second order CorDs together with the diagrams from which it can be calculated. The contribution of the second order CorD approaches zero since they are only made up of one structure and results in a too low power of N_l.
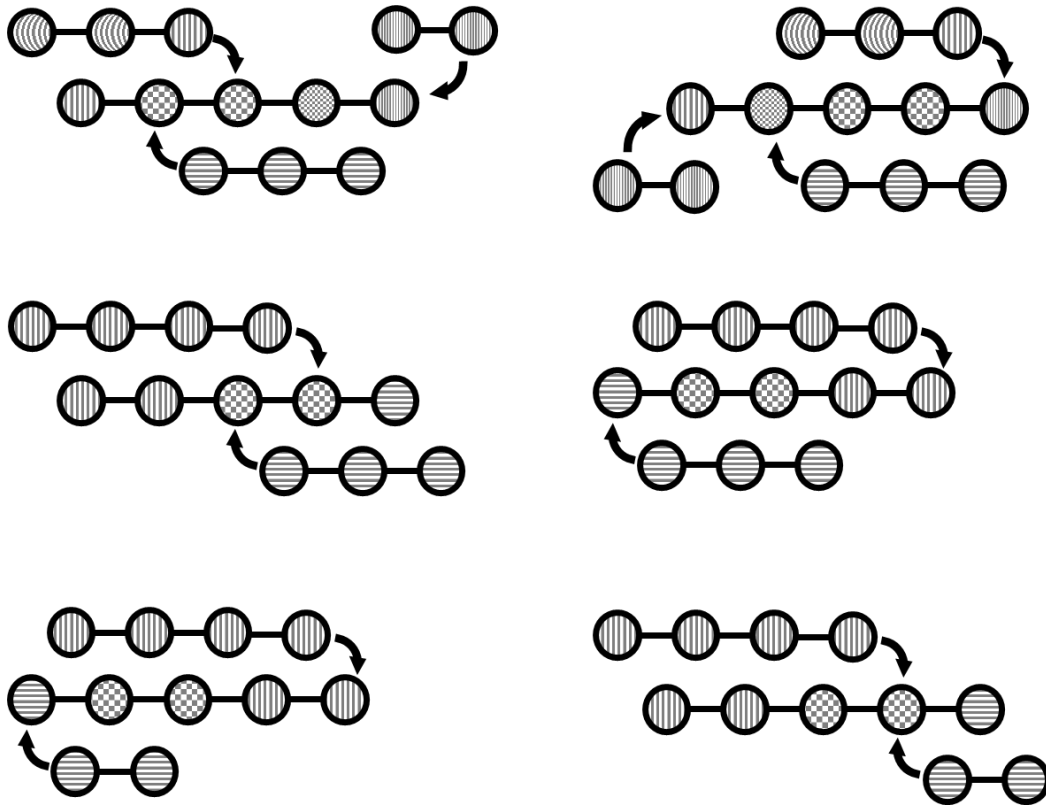
Figure 8: The different ways to overlay the diagrams and form the CorD 4e

Table 4: The pre-factors for the correction diagrams of the second order for the cumulant 5aab₁, with all diagrams the stem from

Correction diagram	Overlaying diagrams with $f_{cd,i}$	Pre-factor f_{cd}
e	bba [-2] cb [2] ca[2]	2
f	bba [-5] ca [2] da [1] cb [4] db [1]	11
g	bba [-6] da [4] db [12]	42
h	bba [-3] ea[2] cb[2]	3
i	bba [-3] ea [2] fa [1] cb [1] db [1]	5
j	bba [-3] ea [1] fa [2] cb [2]	4
k	bba [-5] fa [4] db [2]	5
l	bba [-9] fa [3] ga [1] cb[3] db [1]	6

When naming the individual diagrams, attention was already paid to the correct sequence for placing them. For example, with the 5bba, the first structure b can be placed unhindered because it cannot be completely covered by the structure a. But the positioning takes a possible position for the next structure b, which corresponds to a position $N_{i,j}$ which is eliminated. When placing the structure a, the three positions already occupied by the partial overlapping of two structures b are eliminated. If, however, one of the structures b is placed on another component, no positions for the other b structure and structure a are lost. Both b structures can be freely placed and only two items are left for a. If structure a is placed on a different component than the others, it can be freely positioned. If all three structures are placed on other components, as can happen with tertiary and multiple mixtures, no items are required. In the case of CorDs such as 4ca, structure c can be placed freely again, while structure a has three positions omitted. If there is a structure on another component, no items are omitted. Since the second-order CorDs only consist of one structure, no structures are eliminated. By inserting all the terms determined in this way into equation Eq. 3.35, the equation Eq. 3.38 is obtained for the first cumulant to describe the combinatorial part in case of a system with one component.

$$\gamma_{5bba_1} = \frac{1}{2} * \left(\frac{N_l}{M}\right)^3 * N_b * (N_b - 1) * (N_a - 3)$$

$$- \left(\frac{N_l}{M}\right)^2 * N_c * (N_a - 3) - \left(\frac{N_l}{M}\right)^2 * N_d * (N_a - 3) - \left(\frac{N_l}{M}\right)^2 * N_e * (N_a - 4)$$

$$- \left(\frac{N_l}{M}\right)^2 * N_f * (N_a - 4) - \left(\frac{N_l}{M}\right)^2 * N_g * (N_a - 4) - \left(\frac{N_l}{M}\right)^2 * N_c * (N_b - 2)$$

$$- \left(\frac{N_l}{M}\right)^2 * N_d * (N_b - 3) + \frac{N_l}{M} * N_e + \frac{N_l}{M} * N_f + \frac{N_l}{M} * N_g + \frac{N_l}{M} * N_h$$

$$+ \quad \frac{N_l}{M} * N_i + + \frac{N_l}{M} * N_j + \frac{N_l}{M} * N_k + \frac{N_l}{M} * N_{l,diagram} \qquad \textbf{Eq. 3.38}$$

In the case of the second cumulant 5b|ba$_2$, the structure b is an independent diagram. However, this structure cannot cause any overlapping of vertices and is always independent in every sum without influencing the others in any way. The remaining two structures a and b can therefore only form the structures c and d. This results in the CorDs only the two diagrams {b|c, b|d}. Both are CorDs of the first order. No second order CorDs are therefore formed in this case.

Since neither the cluster diagram nor the CorDs of the cumulant have two identical structures, the pre-factor f$_{eq}$ is one for each sum. The pre-factor f$_{cd}$ is minus two for the diagram b|c because the structures a and b can be placed in the structure c in two ways. For the diagram b|d it is minus three. Since the two diagrams of the cumulant do not influence each other, only the cluster diagram itself has two positions for the structure a. The combinatorial part of the second cumulant thus becomes Eq. 3.39. The entire combinatorial part of the diagram 5bba can therefore be described by the two combinatorial parts of the cumulant.

$$\gamma_{5b|ba_2} = \left(\frac{N_l}{M}\right)^3 * N_b * N_b * (N_a - 2) \; - \; \left(\frac{N_l}{M}\right)^2 * N_b * N_c - \left(\frac{N_l}{M}\right)^2 * N_b * N_d \qquad \textbf{Eq. 3.39}$$

3.4   Energetic mean field

In addition to the entropic diagrams describing all configured micro-states of the system, the energetic diagrams are also needed to describe it completely. These derive from interaction forces between two segments. While the repulsive forces are already considered by the volume contraction, the attractive forces have to be handled separately. Their force is a function of the distance between the segments. In the Flory Huggins theory (FH) (1) only forces between two adjacent segments are considered. If two segments are further separated from each other, the possible interactions are neglected. The interactions can therefore be described by the expression $\delta(r_i, r_j + \alpha_\beta)$, which is already used for the entropic contribution.

This interaction term described by FH Eq. 3.40 is described in the LCT by the linear component of diagram 1a1. This consists of only a single interaction bond between

two segments. The LCT has further energetic diagrams which describe how such interaction bonds behave in combination with other structures. To cover all possible combinations, starting from the entropic diagrams, single existing bonds are replaced by interaction bonds. Like the FH, the LCT also only considers interactions between adjacent segments (16). In diagrams with up to six bonds, up to three of them can be replaced by interactions. The resulting diagrams can describe cases where up to six segments interact simultaneously.

$$Z^{FH} = \exp\left(\sum_{\kappa=1}^{k}\sum_{\lambda=1}\sum_{i \in S_\mu}\sum_{j \in S_\lambda}' \left(\sum_{\beta=1}^{z} \delta\left(r_i, r_j + a_\beta\right) * \varepsilon_{\kappa\lambda}\right)\right)$$ **Eq. 3.40**

The aim of this thesis is to find out whether increasing the number of bonds from four to six has an effect on the predictive power of LCT in small molecules. It is assumed that such an effect can already be determined by developing the necessary entropic contributions. However, a description of the energy is also necessary to describe the system. This is done by the energetic mean field. The energetic mean field neglects all possible combinations of bonds and interactions and considers only the interactions between the adjacent segments. Thus, there are equal interactions between all neighbouring segments. To better understand how much the omission of the energetic diagrams affects the model, the energy has been described in three different ways.

- With the interaction described in the FH, the so-called χ function.

- The energetic mean field used by Freed with up to two interactions.

- A mean field with up to three interactions.

Due to their increase in the number of interaction bonds involved, the maximum order of the interaction parameter also increases. The description with the χ-function has a maximum contribution of $\varepsilon\, z^{-3}$, with Freed's (1) description a maximum contribution of $\varepsilon^2\, z^{-3}$ and with three interaction bonds it is $\varepsilon^2\, z^{-3}$.

The description of the interaction between the individual segments already used in the FH considers only two segments and checks whether an interaction takes place

between them. In the LCT such an interaction is described by diagram 1a1. If an interaction takes place, a potential energy is delivered which is described by interaction parameter $\varepsilon_{\mu,\lambda}$. This parameter describes the interaction between two segments of the components μ and λ. Mathematically it is done by exponential function of multiple sum Eq. 3.40 over all components of the system and all segments of the two selected components. By introducing the Mayer function Eq. 3.41 and multiple transforming this sum becomes the expression Eq. 3.42, which is multiplied to the partition function Z. This product becomes a sum of the logarithms by the logarithm of the partition function Z. The individual products can be lifted out of the logarithm and are transformed into sums. This leaves the two sums of the term in Eq. 3.43.

$$f_{\kappa\lambda} = \exp\left(\varepsilon_{\kappa\lambda} - 1\right) \qquad \text{Eq. 3.41}$$

$$Z^{FH} = \prod_{\kappa=1}^{k}\left(1 + \frac{z}{N_l} * f_{\kappa\kappa}\right)^{\frac{n_\kappa M_\kappa(n_\kappa M_\kappa - 1)}{2!}} * \prod_{\kappa=1}^{k}\prod_{\lambda<\kappa}\left(1 + \frac{z}{N_l} * f_{\kappa\lambda}\right)^{\frac{n_\kappa M_\kappa n_\lambda M_\lambda}{2!}} \qquad \text{Eq. 3.42}$$

$$\ln Z^{FH} = N_l^2 * \left[\sum_{\kappa=1}^{k}\frac{\varphi_\kappa^2}{2} * \ln\left(1 + \frac{z}{N_l} f_{\kappa\kappa}\right) \sum_{\kappa=1}^{k}\sum_{\lambda=1}^{\kappa-1}\varphi_\kappa\varphi_\lambda * \ln\left(1 + \frac{z}{N_l} f_{\kappa\lambda}\right)\right] \qquad \text{Eq. 3.43}$$

Through a series development this term can be further transformed. All but the first term is omitted. When the first term is inserted back into this sum, only the multiple sum Eq. 3.44 remains over the components. The expression of the Mayer function itself can then be transformed again by a series expansion Eq. 3.45, this time a power series expansion. In this model only the linear term of the series is considered, thus the mean field term becomes Eq. 3.46 according to FH. After emphasizing an N_l for the normalization of the free energy, the mean field term can be added to the entropic diagrams as diagram contribution. It falls thereby into the sum linear diagrams $\sum_B C_{Be}^{(\varepsilon)}$ from the sum Eq. 3.47.

$$\ln Z^{FH} = N_l * \frac{z}{2}\sum_{\kappa=1}^{k}\sum_{\lambda=1}^{k}\varphi_\kappa * \varphi_\lambda * f_{\kappa\lambda} \qquad \text{Eq. 3.44}$$

$$f_{\kappa\lambda} = \left(1 + \varepsilon_{\kappa\lambda} + \frac{\varepsilon_{\kappa\lambda}^2}{2} + \frac{\varepsilon_{\kappa\lambda}^3}{6} + \cdots\right) - 1 \qquad \textbf{Eq. 3.45}$$

$$e^{MF} = N_l \frac{z}{2} * \sum_{\kappa=1}^{k} \sum_{\lambda=1}^{k} \varphi_\kappa * \varphi_\lambda * \varepsilon_{\kappa\lambda} \qquad \textbf{Eq. 3.46}$$

$$C_\chi = \frac{z}{2} * \sum_{\kappa=1}^{k} \sum_{\lambda=1}^{k} \varphi_\kappa * \varphi_\lambda * \varepsilon_{\kappa\lambda} \qquad \textbf{Eq. 3.47}$$

The description of the energetic part used by Freed (1) is done via energetic diagrams up to the second order of ε. The energetic mean field is described in this form by diagrams 1a1 and 2b2. Both diagrams are listed in Table 5 and have only interactions between the individual segments. Diagram 1a1 describes the individual interaction between two segments. The contribution of diagram 1a1 is obtained in the same way as the χ-function, by a power series development of the sum Eq. 3.45. The quadratic term is also taken into account here, which leads to two contributions for the diagram 1a1.

Diagram 2b2 on the other hand describes interactions of one segment with two adjacent segments. It represents the diagram 2b where all bonds have been replaced by interaction bonds. The contribution of such an energetic diagram $C_{B,e}$ contains, just like the contribution of an entropic diagram, a lattice-dependent $D_{B,e}$ and a combinatorial part $\gamma_{B,e}$.

The lattice-dependent fraction $D_{B,e}$ can be calculated by Eq. 3.48. The lattice-dependent fraction of the correlating entropic diagram is taken as a starting-point and multiplied by the factor in the square bracket for each replaced bond. This factor is expressed by the first term of a Taylor series development.

$$D_{B,e} = D_{B,m} * \left[\frac{\frac{f_{\kappa\lambda}*z}{N_l}}{1 + \left(f_{\kappa\lambda}*\frac{z}{N_l}\right)}\right]^l = D_{B,m} * \left(\frac{z*\varepsilon_{\kappa\lambda}}{N_l}\right)^l \qquad \textbf{Eq. 3.48}$$

In the case of the 2b2 diagram this results in a lattice-dependent contribution $D_{B,e}$ of Eq. 3.49. The combinatorial contribution $\gamma_{B,e}$ results with Eq. 3.50. It consists of the

symmetry number s_D and the number of possibilities to select the diagram γ_D. The symmetry number s_D corrects the number of ways the diagrams can be found in the selected vertices. It is the reciprocal of the number of ways to connect the selected vertices from one point. In the case of diagram 2b2 there are 2 ways to connect these three interacting vertices from one starting point. The number γ_D in case of diagram 2b2 is the product of the possibilities to select a segment and can be calculated with Eq. 3.51. The number of molecules n_μ can again be represented by the expression Eq. 3.36. The positions which are omitted by previously selected segments do not contribute to the thermodynamic limit and are therefore omitted. The contribution of the diagram results from the product, after the removal of a N_l to normalize the free energy, the thermodynamic limit can be applied. For the diagram b2 this results in the diagram contribution of Eq. 3.52.

$$D_{2b2,e} = \frac{z * \varepsilon_{\kappa\lambda}^3}{N_l^2} \qquad\qquad \textbf{Eq. 3.49}$$

$$\gamma_{B,e} = \gamma_B * s_D \qquad\qquad \textbf{Eq. 3.50}$$

$$\gamma_D = (n_i * M_i)^{N_v} \qquad\qquad \textbf{Eq. 3.51}$$

$$C_{2b2,e} = D_{2b2,e} * \gamma_{2b2,e} = -\frac{z}{2} * \varphi_i^3 * \varepsilon_{\kappa\kappa}^2 \qquad\qquad \textbf{Eq. 3.52}$$

In order to remove interactions between two segments already connected with a bond, Nemirovsky et al. (15) added the term $-\varepsilon$ into the equation Eq. 2.15. These interactions have already been taken into account in the LCT by the bonds themselves. This term can be written into the description of the energetic mean field, thus forming the expression Eq. 3.53.

$$\exp\left(\sum_{\kappa=1}^{k}\sum_{\lambda=1}\sum_{i\in S_\mu}\sum_{j\in S_\lambda}{}' \left(\sum_{\beta=1}^{z} \delta\left(r_i, r_j + a_\beta\right) * \varepsilon_{\kappa\lambda} \right) - \sum_{\kappa=1}^{k}\sum_{\alpha_\kappa=1}^{n_\kappa}\sum_{m_\kappa=1}^{M_\kappa-1} \varepsilon_{\kappa\kappa} \right) \qquad \textbf{Eq. 3.53}$$

Zimmermann et al. (6) introduced another possibility to describe it. All segments already connected by a bond are described by diagram 1a. The product of the number N_a and n_μ describes how often they can be found in the system. In this case N_a describes how often the structure can be found on a chain, and thus how many bonds there are. The number n_μ indicates for a component, how many molecules it has. It is describable by Eq. 3.36. If this structure a is replaced by an interaction, it describes the surplus energetic contribution. As already with the original FH the expression Eq. 3.41 can also be described by the sum Eq. 3.45 by a series development. The corrective term thus appears in both contributions of diagram 1a1. The new contributions are Eq. 3.55 and Eq. 3.56 with the number of lattice sides used for the normalization of the free energy.

$$-\sum_{\kappa=1}^{k} n_\kappa * N_a^{(\kappa)} * \widetilde{\varepsilon_{\kappa\kappa}} = -N_l * \sum_{\kappa=1}^{k} \varphi_\kappa * \frac{N_a^{(\kappa)}}{M_\kappa} * \varepsilon_{\kappa\kappa} \qquad \text{Eq. 3.54}$$

$$C_{1a1,e} = \frac{z}{2} * \varphi_i^2 * \varepsilon_{\kappa\kappa} - \varphi_\kappa * \frac{N_a^{(\kappa)}}{M_\kappa} * \varepsilon_{\kappa\kappa} \qquad \text{Eq. 3.55}$$

$$C_{1a1,e^2} = \frac{z}{4} * \varphi_i^2 * \varepsilon_{\kappa\kappa}^2 - \frac{1}{2} * \varphi_\kappa * \frac{N_a^{(\kappa)}}{M_\kappa} * \varepsilon_{\kappa\kappa}^2 \qquad \text{Eq. 3.56}$$

The third way to describe the energetic part of the LCT is the development of the mean field energy up to the third order. This case corresponds to a maximum contribution of $\varepsilon^3 z^{-3}$. While in the two previous descriptions of the energy, these alone were described by the contributions already known in previous models, this one includes new energetic diagrams. The Mean field is described by the diagrams 1a1, 2b2 and 3c3, which each consist of interaction bonds only. The diagram 2b2 can be taken over unchanged from the previous description and has a contribution from Eq. 3.52. In the diagram 1a1 it is now possible to include the cubic term from the power series, which has a contribution of ε^3. This diagram therefore has three contributions Eq. 3.55, Eq. 3.56 and Eq. 3.57.

$$C_{1a1,e^3} = \frac{z}{12} * \varphi_i^2 * \varepsilon_{\kappa\kappa}^3 - \frac{1}{62} * \varphi_\kappa * \frac{N_a^{(\kappa)}}{M_\kappa} * \varepsilon_{\kappa\kappa}^3 \qquad \text{Eq. 3.57}$$

The contribution of the diagram 3c3 is the same as that of 2b2. Starting from diagram 3c, all its bonds are exchanged by interaction bonds. This is done by multiplying by the first term of the Taylor series development for each exchanged bond with the lattice dependent term $D_{B,e}$. Since the diagram allows four segments to interact and has no bonds, the number of possible placements γ_D is $(n_i * M_i)^4$, ignoring the segment positions that are omitted. The symmetry number s_D is one sixth for four segments. The contribution of the energy diagram 3c3 is therefore Eq. 3.58.

$$C_{3c3,e} = -\frac{z}{6} * \varphi_i^4 * \varepsilon_{\kappa\kappa}^3 \qquad \text{Eq. 3.58}$$

All ways to describe the mean field of energy are based on the interaction parameter $\varepsilon_{\lambda\mu}$. According to Langenbach (12) this parameter can be represented as a series development to describe the temperature dependence of the term. This results in the function Eq. 3.59 for the interaction parameters. This description requires two parameters $\varepsilon_{\lambda\mu,1}$ and $\varepsilon_{\lambda\mu,2}$ which together with the lattice size σ form the parameter set used for the LCT.

$$\varepsilon_{\kappa\lambda} = \frac{\varepsilon_{\kappa\lambda,1}}{k_B T} * \left(1 + \frac{\varepsilon_{\kappa\lambda,2}}{k_B T}\right) \qquad \text{Eq. 3.59}$$

The diagrams required for the individual descriptions of the energetic part of the sum of states are listed again in Table 5 with their respective contributions.

Table 5: All considered energetic diagrams and their contributions for the energetic mean field

Energetic diagram	Contribution $\mathbf{C_{B,e}}$
1a1	$$C_{1a1}^{(\varepsilon)} = \frac{z}{2} \sum_{\kappa=1}^{k} \sum_{\lambda=1}^{k} \varphi_\kappa \varphi_\lambda \varepsilon_{\kappa\lambda} - \sum_{\kappa=1}^{k} \varphi_\kappa \frac{N_a}{M_\kappa} \varepsilon_\kappa$$ $$C_{1a1}^{(\varepsilon^2)} = \frac{z}{4} \sum_{\kappa=1}^{k} \sum_{\lambda=1}^{k} \varphi_\kappa \varphi_\lambda \varepsilon_{\kappa\lambda}^2 - \frac{1}{2} \sum_{\kappa=1}^{k} \varphi_\kappa \frac{N_a}{M_\kappa} \varepsilon_{\kappa\kappa}^2$$ $$C_{1a1}^{(\varepsilon^3)} = \frac{z}{12} \sum_{\kappa=1}^{k} \sum_{\lambda=1}^{k} \varphi_\kappa \varphi_\lambda \varepsilon_{\kappa\lambda}^3 - \frac{1}{6} \sum_{\kappa=1}^{k} \varphi_\kappa \frac{N_a}{M_\kappa} \varepsilon_{\kappa\kappa}^3$$
2b2	$$C_{2b2}^{(\varepsilon^2)} = \frac{z}{2} \sum_{\kappa=1}^{k} \sum_{\lambda=1}^{k} \sum_{\mu=1}^{k} \varphi_\kappa \varphi_\lambda \varphi_\mu \varepsilon_{\kappa\lambda} \, \varepsilon_{\lambda\mu}$$
3c3	$$C_{3c3}^{(\varepsilon^3)} = \frac{z}{2} \sum_{\kappa=1}^{k} \sum_{\lambda=1}^{k} \sum_{\mu=1}^{k} \sum_{\tau=1}^{k} \varphi_\kappa \varphi_\lambda \varphi_\mu \varphi_\tau \varepsilon_{\kappa\lambda} \varepsilon_{\lambda\mu} \varepsilon_{\mu\tau}$$

3.5   Contributions of the entropic diagrams

The contribution of a diagram corrects the mean field from the Flory Huggins depending on the number of times the diagram can be found in the system. By introducing diagrams with up to six bonds, the description of more complex structures in the investigated systems is made possible. In this thesis the entropic diagrams up to the sixth order have been investigated. To describe the mean field of the energy with up to three energetic bonds, the energetic diagrams 1a1, 2b2 and 3c3 are also examined.

The diagram contributions of the individual entropic diagrams result from the product of the combinatorial components and the lattice-dependent components. The combinatorial part indicates how often a diagram can be found in a system. The lattice-dependent fraction indicates how many positions such a diagram can occupy. Diagrams with several structures, diagrams of the second kind have so-called cumulants. These come from the series development of the logarithm and the number of structures indicates their number. Thereby different diagrams are combined which all

together have the same structures as the examined diagram. Each cumulant has a pre-factor which also results from the series development. As you can already see in Eq. 2.7 the pre-factor of the individual terms of the development is significant. The pre-factor of a cumulant f_{cu} also lists how often it can be formed from the individual structures of the diagram. It can be calculated with Eq. 3.60 for each individual cumulant.

$$f_{cu} = k_{ln} * \binom{n_d}{n_{d,f}} * \binom{n_d - n_{d,f}}{n_{d,f,2}} \qquad \text{Eq. 3.60}$$

Here k_{ln} is the pre-factor which it inherits from the term of series expansion. This pre-factor also contains the sign of the cumulant. n_d is the number of different diagrams in the cumulant and $n_{d,f}$ is the number of the most frequent diagram. If there are more than two different diagrams, the binomial coefficient is determined from the remaining diagrams and multiplied. To get the amount of a diagram, you must determine the sum of all the cumulants.

The Helmholtz energy expressed with the model is still dependent on the system size in the description. In order to normalize it and make it independent of it, the Helmholtz energy must be divided by the number of lattice positions. In the contributions this is expressed by the extraction and subsequent division by the number of lattice sites N_l.

The resulting contribution of the diagram itself contains many terms which are divided several times by the number of lattice sites. Such a lattice site corresponds to a discretized location for a segment. A macroscopic system contains a huge number of possible locations for each segment. To take this huge number into account in the model, the thermodynamic limit is applied. The value N_l which represents the number of lattice locations is set to infinity and all terms in the with it in the denominator become infinitely small. If a term would have the expression in the numerator, its contribution would be infinite. This should not happen and would indicate an error in the development of the contribution. The remaining terms correspond to the contribution of the diagram and can be read in Table 6 for all diagrams considered in this thesis.

3.5.1 Example 5bba

As already described in the description of the determination of the lattice-dependent and combinatorial components, the determination of the diagram contribution itself is also carried out exemplarily. Here the diagram 5bba is chosen. It has two cumulants, each with a combinatorial and a lattice-dependent component. By multiplying these two terms, you obtain the diagram contributions of the individual cumulants.

These can be multiplied by their respective pre-factors. The pre-factor for the first cumulant $5bba_1$ is one, since both the factor k from the series development and the number of diagrams in the cumulant are one. For $5b|ba_2$, the contribution is minus one, because although the factor k is minus 0.5, the cumulant also has two identical diagrams. From the sum of the two cumulants, the number of lattice locations N_l is now extracted to normalize the free energy. The resulting contribution of the diagram still contains many terms with N_l in the denominator. A large part of these are derived from the polynomials of the omitted positions. After applying the thermodynamic limit, these terms become zero and only the contribution remains for the diagram.

3.5.2 List of the contributions

Table 6: The contribution of all inspected cluster diagrams

1a	$C_{1a}^{(s)} = 0$	**2b**	$C_{2b}^{(s)} = -\dfrac{1}{z}\sum_{\mu=1}^{2}\dfrac{N_a}{M_\mu}\varphi_\mu$

2aa $\quad C_{2aa}^{(s)} = \dfrac{1}{z}\sum_{\mu=1}^{2}\sum_{\kappa=1}^{2}\dfrac{N_a}{M_\mu}\dfrac{N_a}{M_\kappa}\varphi_\mu\varphi_\kappa$
$\qquad\qquad$ **3c** $\quad C_{3c}^{(s)} = \dfrac{1}{z^2}\sum_{\mu=1}^{2}\dfrac{N_c}{M_\mu}\varphi_\mu$

3d $\quad C_{3d}^{(s)} = \dfrac{2}{z^2}\sum_{\mu=1}^{2}\dfrac{N_d}{M_\mu}\varphi_\mu$
$\qquad\qquad$ **3aaa** $\quad C_{3aaa}^{(s)} = \dfrac{8}{3z^2}\sum_{\mu=1}^{2}\sum_{\kappa=1}^{2}\sum_{\lambda=1}^{2}\dfrac{N_a}{M_\mu}\dfrac{N_a}{M_\kappa}\dfrac{N_a}{M_\lambda}\varphi_\mu\varphi_\kappa\varphi_\lambda$

3ba $\quad C_{3ba}^{(s)} = -\dfrac{4}{z^2}\sum_{\mu=1}^{2}\sum_{\kappa=1}^{2}\dfrac{N_b}{M_\mu}\dfrac{N_a}{M_\kappa}\varphi_\mu\varphi_\kappa$
$\qquad\qquad$ **4e** $\quad C_{4e}^{(s)} = \dfrac{1}{z^3}\sum_{\mu=1}^{2}\dfrac{N_e}{M_\mu}\varphi_\mu$

4f $\quad C_{4f}^{(s)} = \dfrac{1}{z^2}\sum_{\mu=1}^{2}\dfrac{N_f}{M_\mu}\varphi_\mu - \dfrac{2}{z^3}\sum_{\mu=1}^{2}\dfrac{N_f}{M_\mu}\varphi_\mu$
$\qquad$ **4g** $\quad C_{4g}^{(s)} = \dfrac{3}{z^2}\sum_{\mu=1}^{2}\dfrac{N_g}{M_\mu}\varphi_\mu - \dfrac{6}{z^2}\sum_{\mu=1}^{2}\dfrac{N_g}{M_\mu}\varphi_\mu$

4aaaa
$$C_{4aaaa}^{(s)} = \frac{2}{z^2}\sum_{\mu}^{2}\sum_{\kappa}^{2}\sum_{\lambda}^{2}\sum_{\tau}^{2}\frac{N_a}{M_\mu}\frac{N_a}{M_\kappa}\frac{N_a}{M_\lambda}\frac{N_a}{M_\tau}\varphi_\mu\varphi_\kappa\varphi_\lambda\varphi_\tau + \frac{6}{z^3}\sum_{\mu}^{2}\sum_{\kappa}^{2}\sum_{\lambda}^{2}\sum_{\tau}^{2}\frac{N_a}{M_\mu}\frac{N_a}{M_\kappa}\frac{N_a}{M_\lambda}\frac{N_a}{M_\tau}\varphi_\mu\varphi_\kappa\varphi_\lambda\varphi_\tau$$
$$-\frac{2}{z^2}\sum_{\mu=1}^{2}\sum_{\kappa=1}^{2}\sum_{\lambda=1}^{2}\frac{N_a}{M_\mu}\frac{N_a}{M_\kappa}\frac{N_a}{M_\lambda}\varphi_\mu\varphi_\kappa\varphi_\lambda - \frac{4}{z^2}\sum_{\mu}^{2}\sum_{\kappa}^{2}\sum_{\lambda}^{2}\frac{N_b}{M_\mu}\frac{N_a}{M_\kappa}\frac{N_a}{M_\lambda}\varphi_\mu\varphi_\kappa\varphi_\lambda$$

4baa
$$C_{4baa}^{(s)} = -\frac{12}{z^3}\sum_{\mu}^{2}\sum_{\kappa}^{2}\sum_{\lambda}^{2}\frac{N_b}{M_\mu}\frac{N_a}{M_\kappa}\frac{N_a}{M_\lambda}\varphi_\mu\varphi_\kappa\varphi_\lambda + \frac{4}{z^2}\sum_{\mu=1}^{2}\sum_{\kappa=1}^{2}\frac{N_b}{M_\mu}\frac{N_a}{M_\kappa}\varphi_\mu\varphi_\kappa + \frac{4}{z^2}\sum_{\mu}^{2}\sum_{\kappa}^{2}\frac{N_c}{M_\mu}\frac{N_a}{M_\kappa}\varphi_\mu\varphi_\kappa$$
$$+\frac{6}{z^2}\sum_{\mu}^{2}\sum_{\kappa}^{2}\frac{N_d}{M_\mu}\frac{N_a}{M_\kappa}\varphi_\mu\varphi_\kappa$$

4ca $\quad C_{4ca}^{(s)} = -\dfrac{2}{z^2}\sum_{\mu}^{2}\sum_{\kappa}^{2}\dfrac{N_c}{M_\mu}\dfrac{N_a}{M_\kappa}\varphi_\mu\varphi_\kappa + \dfrac{2}{z^3}\sum_{\mu}^{2}\sum_{\kappa}^{2}\dfrac{N_c}{M_\mu}\dfrac{N_a}{M_\kappa}\varphi_\mu\varphi_\kappa$

4da $\quad C_{4da}^{(s)} = -\dfrac{6}{z^2}\sum_{\mu}^{2}\sum_{\kappa}^{2}\dfrac{N_d}{M_\mu}\dfrac{N_a}{M_\kappa}\varphi_\mu\varphi_\kappa + \dfrac{12}{z^2}\sum_{\mu}^{2}\sum_{\kappa}^{2}\dfrac{N_d}{M_\mu}\dfrac{N_a}{M_\kappa}\varphi_\mu\varphi_\kappa$

4bb
$$C_{4bb}^{(s)} = \frac{1}{z^2}\sum_{\mu}^{2}\sum_{\kappa}^{2}\frac{N_b}{M_\mu}\frac{N_b}{M_\kappa}\varphi_\mu\varphi_\kappa + \frac{2}{z^2}\sum_{\mu}^{2}\sum_{\kappa}^{2}\frac{N_b}{M_\mu}\frac{N_b}{M_\kappa}\varphi_\mu\varphi_\kappa - \frac{1}{2z^2}\sum_{\mu=1}^{2}\frac{N_b}{M_\mu}\varphi_\mu - \frac{1}{z^2}\sum_{\mu=1}^{2}\frac{N_c}{M_\mu}\varphi_\mu \quad \frac{3}{z^2}\sum_{\mu=1}^{2}\frac{N_d}{M_\mu}\varphi_\mu - \frac{1}{z^2}\sum_{\mu=1}^{2}\frac{N_e}{M_\mu}\varphi_\mu$$
$$-\frac{1}{z^2}\sum_{\mu=1}^{2}\frac{N_f}{M_\mu}\varphi_\mu - \frac{3}{z^2}\sum_{\mu=1}^{2}\frac{N_g}{M_\mu}\varphi_\mu$$

5h	$C_{5h}^{(s)} = \dfrac{1}{z^3}\sum_{\mu=1}^{2}\dfrac{N_h}{M_\mu}\varphi_\mu$	**5i**	$C_{5i}^{(s)} = \dfrac{1}{z^3}\sum_{\mu=1}^{2}\dfrac{N_i}{M_\mu}\varphi_\mu$
5j	$C_{5j}^{(s)} = 0$	**5k**	$C_{5k}^{(s)} = -\dfrac{4}{z^3}\sum_{\mu=1}^{2}\dfrac{N_k}{M_\mu}\varphi_\mu$

5l $\quad C_{5l}^{(s)} = -\dfrac{5}{z^3}\sum_{\mu=1}^{2}\dfrac{N_l}{M_\mu}\varphi_\mu$

5aaaaa
$$C_{5aaaaa}^{(s)} = -\frac{144}{z^3}\sum_{\mu=1}^{2}\sum_{\kappa=1}^{2}\sum_{\lambda=1}^{2}\sum_{\tau=1}^{2}\sum_{\omega=1}^{2}\frac{N_a}{M_\mu}\frac{N_a}{M_\kappa}\frac{N_a}{M_\lambda}\frac{N_a}{M_\tau}\frac{N_a}{M_\omega}\varphi_\mu\varphi_\kappa\varphi_\lambda\varphi_\tau\varphi_\omega \quad -\frac{16}{z^3}\sum_{\mu}^{2}\sum_{\kappa}^{2}\sum_{\lambda}^{2}\sum_{\tau}^{2}\frac{N_a}{M_\mu}\frac{N_a}{M_\kappa}\frac{N_a}{M_\lambda}\frac{N_a}{M_\tau}\varphi_\mu\varphi_\kappa\varphi_\lambda\varphi_\tau$$
$$-\frac{32}{z^3}\sum_{\mu}^{2}\sum_{\kappa}^{2}\sum_{\lambda}^{2}\frac{N_b}{M_\mu}\frac{N_a}{M_\kappa}\frac{N_a}{M_\lambda}\varphi_\mu\varphi_\kappa\varphi_\lambda$$

5baaa
$$C_{5baaa}^{(s)} = -\frac{48}{z^3}\sum_{\mu}^{2}\sum_{\kappa}^{2}\sum_{\lambda}^{2}\sum_{\tau}^{2}\frac{N_b}{M_\mu}\frac{N_a}{M_\kappa}\frac{N_a}{M_\lambda}\frac{N_a}{M_\tau}\varphi_\mu\varphi_\kappa\varphi_\lambda\varphi_\tau + \frac{40}{z^3}\sum_{\mu}^{2}\sum_{\kappa}^{2}\sum_{\lambda}^{2}\frac{N_b}{M_\mu}\frac{N_a}{M_\kappa}\frac{N_a}{M_\lambda}\varphi_\mu\varphi_\kappa\varphi_\lambda$$
$$+\frac{16}{z^3}\sum_{\mu}^{2}\sum_{\kappa}^{2}\sum_{\lambda}^{2}\frac{N_b}{M_\mu}\frac{N_b}{M_\kappa}\frac{N_a}{M_\lambda}\varphi_\mu\varphi_\kappa\varphi_\lambda + \frac{32}{z^3}\sum_{\mu}^{2}\sum_{\kappa}^{2}\sum_{\lambda}^{2}\frac{N_c}{M_\mu}\frac{N_a}{M_\kappa}\frac{N_a}{M_\lambda}\varphi_\mu\varphi_\kappa\varphi_\lambda$$
$$+\frac{48}{z^3}\sum_{\mu}^{2}\sum_{\kappa}^{2}\sum_{\lambda}^{2}\frac{N_b}{M_\mu}\frac{N_a}{M_\kappa}\frac{N_a}{M_\lambda}\varphi_\mu\varphi_\kappa\varphi_\lambda$$

5caa
$$C_{5caa}^{(s)} = +\frac{4}{z^3}\sum_{\mu}^{2}\sum_{\kappa}^{2}\sum_{\lambda}^{2}\frac{N_c}{M_\mu}\frac{N_a}{M_\kappa}\frac{N_a}{M_\lambda}\varphi_\mu\varphi_\kappa\varphi_\lambda \quad -\frac{6}{z^3}\sum_{\mu=1}^{2}\sum_{\kappa=1}^{2}\frac{N_c}{M_\mu}\frac{N_a}{M_\kappa}\varphi_\mu\varphi_\kappa \quad -\frac{4}{z^3}\sum_{\mu=1}^{2}\sum_{\kappa=1}^{2}\frac{N_e}{M_\mu}\frac{N_a}{M_\kappa}\varphi_\mu\varphi_\kappa$$
$$-\frac{4}{z^3}\sum_{\mu=1}^{2}\sum_{\kappa=1}^{2}\frac{N_f}{M_\mu}\frac{N_a}{M_\kappa}\varphi_\mu\varphi_\kappa$$

5daa
$$C_{5daa}^{(s)} = -\frac{24}{z^3}\sum_{\mu}^{2}\sum_{\kappa}^{2}\sum_{\lambda}^{2}\frac{N_d}{M_\mu}\frac{N_a}{M_\kappa}\frac{N_a}{M_\lambda}\varphi_\mu\varphi_\kappa\varphi_\lambda \quad -\frac{12}{z^3}\sum_{\mu=1}^{2}\sum_{\kappa=1}^{2}\frac{N_d}{M_\mu}\frac{N_a}{M_\kappa}\varphi_\mu\varphi_\kappa \quad -\frac{4}{z^3}\sum_{\mu=1}^{2}\sum_{\kappa=1}^{2}\frac{N_f}{M_\mu}\frac{N_a}{M_\kappa}\varphi_\mu\varphi_\kappa$$
$$-\frac{16}{z^3}\sum_{\mu=1}^{2}\sum_{\kappa=1}^{2}\frac{N_g}{M_\mu}\frac{N_a}{M_\kappa}\varphi_\mu\varphi_\kappa$$

5ea
$$C_{5ea}^{(s)} = -\frac{4}{z^3}\sum_{\mu=1}^{2}\sum_{\kappa=1}^{2}\frac{N_e}{M_\mu}\frac{N_a}{M_\kappa}\varphi_\mu\varphi_\kappa$$

5fa
$$C_{5fa}^{(s)} = \frac{8}{z^3}\sum_{\mu=1}^{2}\sum_{\kappa=1}^{2}\frac{N_f}{M_\mu}\frac{N_a}{M_\kappa}\varphi_\mu\varphi_\kappa$$

5ga
$$C_{5ga}^{(s)} = \frac{40}{z^3}\sum_{\mu=1}^{2}\sum_{\kappa=1}^{2}\frac{N_g}{M_\mu}\frac{N_a}{M_\kappa}\varphi_\mu\varphi_\kappa$$

5bba
$$C_{5bba}^{(s)} = \frac{8}{z^3}\sum_{\mu}^{2}\sum_{\kappa}^{2}\sum_{\lambda}^{2}\frac{N_b}{M_\mu}\frac{N_b}{M_\kappa}\frac{N_a}{M_\lambda}\varphi_\mu\varphi_\kappa\varphi_\lambda \quad -\frac{4}{z^3}\sum_{\mu=1}^{2}\sum_{\kappa=1}^{2}\frac{N_b}{M_\mu}\frac{N_a}{M_\kappa}\varphi_\mu\varphi_\kappa \quad -\frac{4}{z^3}\sum_{\mu=1}^{2}\sum_{\kappa=1}^{2}\frac{N_b}{M_\mu}\frac{N_b}{M_\kappa}\varphi_\mu\varphi_\kappa$$
$$-\frac{8}{z^3}\sum_{\mu=1}^{2}\sum_{\kappa=1}^{2}\frac{N_c}{M_\mu}\frac{N_a}{M_\kappa}\varphi_\mu\varphi_\kappa \quad -\frac{24}{z^3}\sum_{\mu=1}^{2}\sum_{\kappa=1}^{2}\frac{N_d}{M_\mu}\frac{N_a}{M_\kappa}\varphi_\mu\varphi_\kappa \quad -\frac{8}{z^3}\sum_{\mu=1}^{2}\sum_{\kappa=1}^{2}\frac{N_e}{M_\mu}\frac{N_a}{M_\kappa}\varphi_\mu\varphi_\kappa$$
$$-\frac{8}{z^2}\sum_{\mu=1}^{2}\sum_{\kappa=1}^{2}\frac{N_f}{M_\mu}\frac{N_a}{M_\kappa}\varphi_\mu\varphi_\kappa \quad -\frac{24}{z^3}\sum_{\mu=1}^{2}\sum_{\kappa=1}^{2}\frac{N_g}{M_\mu}\frac{N_a}{M_\kappa}\varphi_\mu\varphi_\kappa \quad -\frac{8}{z^3}\sum_{\mu=1}^{2}\sum_{\kappa=1}^{2}\frac{N_c}{M_\mu}\frac{N_b}{M_\kappa}\varphi_\mu\varphi_\kappa$$
$$-\frac{12}{z^3}\sum_{\mu=1}^{2}\sum_{\kappa=1}^{2}\frac{N_d}{M_\mu}\frac{N_b}{M_\kappa}\varphi_\mu\varphi_\kappa$$

5cb
$$C_{5cb}^{(s)} = -\frac{4}{z^3}\sum_{\mu=1}^{2}\sum_{\kappa=1}^{2}\frac{N_c}{M_\mu}\frac{N_b}{M_\kappa}\varphi_\mu\varphi_\kappa \quad +\frac{2}{z^3}\sum_{\mu=1}^{2}\frac{N_c}{M_\mu}\varphi_\mu +\frac{2}{z^3}\sum_{\mu=1}^{2}\frac{N_e}{M_\mu}\varphi_\mu +\frac{4}{z^3}\sum_{\mu=1}^{2}\frac{N_f}{M_\mu}\varphi_\mu +\frac{2}{z^3}\sum_{\mu=1}^{2}\frac{N_h}{M_\mu}\varphi_\mu +\frac{1}{z^3}\sum_{\mu=1}^{2}\frac{N_i}{M_\mu}\varphi_\mu$$
$$+\frac{2}{z^3}\sum_{\mu=1}^{2}\frac{N_j}{M_\mu}\varphi_\mu +\frac{3}{z^3}\sum_{\mu=1}^{2}\frac{N_l}{M_\mu}\varphi_\mu$$

5db
$$C_{5db}^{(s)} = -\frac{24}{z^3}\sum_{\mu=1}^{2}\sum_{\kappa=1}^{2}\frac{N_d}{M_\mu}\frac{N_b}{M_\kappa}\varphi_\mu\varphi_\kappa \quad +\frac{6}{z^3}\sum_{\mu=1}^{2}\frac{N_d}{M_\mu}\varphi_\mu +\frac{2}{z^3}\sum_{\mu=1}^{2}\frac{N_f}{M_\mu}\varphi_\mu +\frac{24}{z^3}\sum_{\mu=1}^{2}\frac{N_g}{M_\mu}\varphi_\mu +\frac{2}{z^3}\sum_{\mu=1}^{2}\frac{N_i}{M_\mu}\varphi_\mu +\frac{2}{z^3}\sum_{\mu=1}^{2}\frac{N_k}{M_\mu}\varphi_\mu$$
$$+\frac{4}{z^3}\sum_{\mu=1}^{2}\frac{N_l}{M_\mu}\varphi_\mu$$

6m
$$C_{6m}^{(s)} = -\frac{3}{z^3}\sum_{\mu=1}^{2}\frac{N_m}{M_\mu}\varphi_\mu$$

6n $\quad C_{6n}^{(s)} = 0$

6o $C_{6o}^{(s)} = 0$ **6p** $C_{6p}^{(s)} = -\dfrac{1}{z^3}\sum_{\mu=1}^{2}\dfrac{N_p}{M_\mu}\varphi_\mu$

6q $C_{6q}^{(s)} = \dfrac{1}{z^3}\sum_{\mu=1}^{2}\dfrac{N_q}{M_\mu}\varphi_\mu$ **6r** $C_{6r}^{(s)} = 0$

6s $C_{6s}^{(s)} = 0$ **6t** $C_{6t}^{(s)} = -\dfrac{3}{z^3}\sum_{\mu=1}^{2}\dfrac{N_t}{M_\mu}\varphi_\mu$

6u $C_{6u}^{(s)} = \dfrac{2}{z^3}\sum_{\mu=1}^{2}\dfrac{N_u}{M_\mu}\varphi_\mu$

6aaaaaa

$$
\begin{aligned}
C_{6aaaaaa}^{(s)} =\;& \frac{64}{z^3}\sum_{\mu=1}^{2}\sum_{\kappa=1}^{2}\sum_{\lambda=1}^{2}\sum_{\tau=1}^{2}\sum_{\omega=1}^{2}\sum_{\upsilon=1}^{2}\frac{N_a}{M_\mu}\frac{N_a}{M_\kappa}\frac{N_a}{M_\lambda}\frac{N_a}{M_\tau}\frac{N_a}{M_\omega}\frac{N_a}{M_\upsilon}\varphi_\mu\varphi_\kappa\varphi_\lambda\varphi_\tau\varphi_\omega\varphi_\upsilon \\
& -\frac{16}{z^3}\sum_{\mu=1}^{2}\sum_{\kappa=1}^{2}\sum_{\lambda=1}^{2}\sum_{\tau=1}^{2}\sum_{\omega=1}^{2}\frac{N_a}{M_\mu}\frac{N_a}{M_\kappa}\frac{N_a}{M_\lambda}\frac{N_a}{M_\tau}\frac{N_a}{M_\omega}\varphi_\mu\varphi_\kappa\varphi_\lambda\varphi_\tau\varphi_\omega \\
& -\frac{32}{z^3}\sum_{\mu=1}^{2}\sum_{\kappa=1}^{2}\sum_{\lambda=1}^{2}\sum_{\tau=1}^{2}\sum_{\omega=1}^{2}\frac{N_b}{M_\mu}\frac{N_a}{M_\kappa}\frac{N_a}{M_\lambda}\frac{N_a}{M_\tau}\frac{N_a}{M_\omega}\varphi_\mu\varphi_\kappa\varphi_\lambda\varphi_\tau\varphi_\omega \\
& +\frac{20}{3z^3}\sum_{\mu}^{2}\sum_{\kappa}^{2}\sum_{\lambda}^{2}\sum_{\tau}^{2}\frac{N_a}{M_\mu}\frac{N_a}{M_\kappa}\frac{N_a}{M_\lambda}\frac{N_a}{M_\tau}\varphi_\mu\varphi_\kappa\varphi_\lambda\varphi_\tau + \frac{32}{z^3}\sum_{\mu}^{2}\sum_{\kappa}^{2}\sum_{\lambda}^{2}\sum_{\tau}^{2}\frac{N_b}{M_\mu}\frac{N_a}{M_\kappa}\frac{N_a}{M_\lambda}\frac{N_a}{M_\tau}\varphi_\mu\varphi_\kappa\varphi_\lambda\varphi_\tau \\
& +\frac{16}{z^3}\sum_{\mu}^{2}\sum_{\kappa}^{2}\sum_{\lambda}^{2}\sum_{\tau}^{2}\frac{N_b}{M_\mu}\frac{N_b}{M_\kappa}\frac{N_a}{M_\lambda}\frac{N_a}{M_\tau}\varphi_\mu\varphi_\kappa\varphi_\lambda\varphi_\tau + \frac{8}{z^3}\sum_{\mu}^{2}\sum_{\kappa}^{2}\sum_{\lambda}^{2}\sum_{\tau}^{2}\frac{N_c}{M_\mu}\frac{N_a}{M_\kappa}\frac{N_a}{M_\lambda}\frac{N_a}{M_\tau}\varphi_\mu\varphi_\kappa\varphi_\lambda\varphi_\tau \\
& +\frac{16}{z^3}\sum_{\mu}^{2}\sum_{\kappa}^{2}\sum_{\lambda}^{2}\sum_{\tau}^{2}\frac{N_d}{M_\mu}\frac{N_a}{M_\kappa}\frac{N_a}{M_\lambda}\frac{N_a}{M_\tau}\varphi_\mu\varphi_\kappa\varphi_\lambda\varphi_\tau
\end{aligned}
$$

6baaaa

$$
\begin{aligned}
C_{6baaaa}^{(s)} =\;& \frac{141}{z^3}\sum_{\mu=1}^{2}\sum_{\kappa=1}^{2}\sum_{\lambda=1}^{2}\sum_{\tau=1}^{2}\sum_{\omega=1}^{2}\frac{N_b}{M_\mu}\frac{N_a}{M_\kappa}\frac{N_a}{M_\lambda}\frac{N_a}{M_\tau}\frac{N_a}{M_\omega}\varphi_\mu\varphi_\kappa\varphi_\lambda\varphi_\tau\varphi_\omega + \frac{16}{z^3}\sum_{\mu}^{2}\sum_{\kappa}^{2}\sum_{\lambda}^{2}\sum_{\tau}^{2}\frac{N_b}{M_\mu}\frac{N_a}{M_\kappa}\frac{N_a}{M_\lambda}\frac{N_a}{M_\tau}\varphi_\mu\varphi_\kappa\varphi_\lambda\varphi_\tau \\
& +\frac{16}{z^3}\sum_{\mu}^{2}\sum_{\kappa}^{2}\sum_{\lambda}^{2}\sum_{\tau}^{2}\frac{N_c}{M_\mu}\frac{N_a}{M_\kappa}\frac{N_a}{M_\lambda}\frac{N_a}{M_\tau}\varphi_\mu\varphi_\kappa\varphi_\lambda\varphi_\tau + \frac{24}{z^3}\sum_{\mu}^{2}\sum_{\kappa}^{2}\sum_{\lambda}^{2}\sum_{\tau}^{2}\frac{N_d}{M_\mu}\frac{N_a}{M_\kappa}\frac{N_a}{M_\lambda}\frac{N_a}{M_\tau}\varphi_\mu\varphi_\kappa\varphi_\lambda\varphi_\tau \\
& -\frac{24}{z^3}\sum_{\mu}^{2}\sum_{\kappa}^{2}\sum_{\lambda}^{2}\frac{N_b}{M_\mu}\frac{N_a}{M_\kappa}\frac{N_a}{M_\lambda}\varphi_\mu\varphi_\kappa\varphi_\lambda - \frac{4}{z^3}\sum_{\mu}^{2}\sum_{\kappa}^{2}\sum_{\lambda}^{2}\frac{N_b}{M_\mu}\frac{N_b}{M_\kappa}\frac{N_a}{M_\lambda}\varphi_\mu\varphi_\kappa\varphi_\lambda \\
& -\frac{6}{z^3}\sum_{\mu}^{2}\sum_{\kappa}^{2}\sum_{\lambda}^{2}\frac{N_b}{M_\mu}\frac{N_b}{M_\kappa}\frac{N_b}{M_\lambda}\varphi_\mu\varphi_\kappa\varphi_\lambda - \frac{38}{z^3}\sum_{\mu}^{2}\sum_{\kappa}^{2}\sum_{\lambda}^{2}\frac{N_c}{M_\mu}\frac{N_a}{M_\kappa}\frac{N_a}{M_\lambda}\varphi_\mu\varphi_\kappa\varphi_\lambda \\
& -\frac{66}{z^3}\sum_{\mu}^{2}\sum_{\kappa}^{2}\sum_{\lambda}^{2}\frac{N_d}{M_\mu}\frac{N_a}{M_\kappa}\frac{N_a}{M_\lambda}\varphi_\mu\varphi_\kappa\varphi_\lambda - \frac{12}{z^3}\sum_{\mu}^{2}\sum_{\kappa}^{2}\sum_{\lambda}^{2}\frac{N_e}{M_\mu}\frac{N_a}{M_\kappa}\frac{N_a}{M_\lambda}\varphi_\mu\varphi_\kappa\varphi_\lambda \\
& -\frac{20}{z^3}\sum_{\mu}^{2}\sum_{\kappa}^{2}\sum_{\lambda}^{2}\frac{N_f}{M_\mu}\frac{N_a}{M_\kappa}\frac{N_a}{M_\lambda}\varphi_\mu\varphi_\kappa\varphi_\lambda - \frac{48}{z^3}\sum_{\mu}^{2}\sum_{\kappa}^{2}\sum_{\lambda}^{2}\frac{N_g}{M_\mu}\frac{N_a}{M_\kappa}\frac{N_a}{M_\lambda}\varphi_\mu\varphi_\kappa\varphi_\lambda \\
& -\frac{16}{z^3}\sum_{\mu}^{2}\sum_{\kappa}^{2}\sum_{\lambda}^{2}\frac{N_c}{M_\mu}\frac{N_b}{M_\kappa}\frac{N_a}{M_\lambda}\varphi_\mu\varphi_\kappa\varphi_\lambda - \frac{24}{z^3}\sum_{\mu}^{2}\sum_{\kappa}^{2}\sum_{\lambda}^{2}\frac{N_d}{M_\mu}\frac{N_b}{M_\kappa}\frac{N_a}{M_\lambda}\varphi_\mu\varphi_\kappa\varphi_\lambda
\end{aligned}
$$

6caaa

$$
\begin{aligned}
C_{6caaa}^{(s)} =\;& +\frac{8}{z^3}\sum_{\mu}^{2}\sum_{\kappa}^{2}\sum_{\lambda}^{2}\sum_{\tau}^{2}\frac{N_c}{M_\mu}\frac{N_a}{M_\kappa}\frac{N_a}{M_\lambda}\frac{N_a}{M_\tau}\varphi_\mu\varphi_\kappa\varphi_\lambda\varphi_\tau + \frac{16}{z^3}\sum_{\mu}^{2}\sum_{\kappa}^{2}\sum_{\lambda}^{2}\frac{N_c}{M_\mu}\frac{N_a}{M_\kappa}\frac{N_a}{M_\lambda}\varphi_\mu\varphi_\kappa\varphi_\lambda \\
& +\frac{8}{z^3}\sum_{\mu}^{2}\sum_{\kappa}^{2}\sum_{\lambda}^{2}\frac{N_e}{M_\mu}\frac{N_a}{M_\kappa}\frac{N_a}{M_\lambda}\varphi_\mu\varphi_\kappa\varphi_\lambda + \frac{8}{z^3}\sum_{\mu}^{2}\sum_{\kappa}^{2}\sum_{\lambda}^{2}\frac{N_f}{M_\mu}\frac{N_a}{M_\kappa}\frac{N_a}{M_\lambda}\varphi_\mu\varphi_\kappa\varphi_\lambda \\
& +\frac{8}{z^3}\sum_{\mu}^{2}\sum_{\kappa}^{2}\sum_{\lambda}^{2}\frac{N_c}{M_\mu}\frac{N_b}{M_\kappa}\frac{N_a}{M_\lambda}\varphi_\mu\varphi_\kappa\varphi_\lambda
\end{aligned}
$$

6daaa
$$C_{6daaa}^{(s)} = -\frac{40}{z^3} \sum_\mu^2 \sum_\kappa^2 \sum_\lambda^2 \sum_\tau^2 \frac{N_d}{M_\mu} \frac{N_a}{M_\kappa} \frac{N_a}{M_\lambda} \frac{N_a}{M_\tau} \varphi_\mu \varphi_\kappa \varphi_\lambda \varphi_\tau + \frac{48}{z^3} \sum_\mu^2 \sum_\kappa^2 \sum_\lambda^2 \frac{N_d}{M_\mu} \frac{N_a}{M_\kappa} \frac{N_a}{M_\lambda} \varphi_\mu \varphi_\kappa \varphi_\lambda$$
$$+ \frac{12}{z^3} \sum_\mu^2 \sum_\kappa^2 \sum_\lambda^2 \frac{N_f}{M_\mu} \frac{N_a}{M_\kappa} \frac{N_a}{M_\lambda} \varphi_\mu \varphi_\kappa \varphi_\lambda + \frac{48}{z^3} \sum_\mu^2 \sum_\kappa^2 \sum_\lambda^2 \frac{N_g}{M_\mu} \frac{N_a}{M_\kappa} \frac{N_a}{M_\lambda} \varphi_\mu \varphi_\kappa \varphi_\lambda$$
$$+ \frac{24}{z^3} \sum_\mu^2 \sum_\kappa^2 \sum_\lambda^2 \frac{N_d}{M_\mu} \frac{N_b}{M_\kappa} \frac{N_a}{M_\lambda} \varphi_\mu \varphi_\kappa \varphi_\lambda$$

6eaa $\quad C_{6eaa}^{(s)} = 0$

6faa
$$C_{6faa}^{(s)} = -\frac{8}{z^3} \sum_\mu^2 \sum_\kappa^2 \frac{N_f}{M_\mu} \frac{N_a}{M_\kappa} \varphi_\mu \varphi_\kappa - \frac{2}{z^3} \sum_\mu^2 \sum_\kappa^2 \frac{N_i}{M_\mu} \frac{N_a}{M_\kappa} \varphi_\mu \varphi_\kappa - \frac{4}{z^3} \sum_\mu^2 \sum_\kappa^2 \frac{N_j}{M_\mu} \frac{N_a}{M_\kappa} \varphi_\mu \varphi_\kappa - \frac{8}{z^3} \sum_\mu^2 \sum_\kappa^2 \frac{N_k}{M_\mu} \frac{N_a}{M_\kappa} \varphi_\mu \varphi_\kappa$$
$$- \frac{6}{z^3} \sum_\mu^2 \sum_\kappa^2 \frac{N_l}{M_\mu} \frac{N_a}{M_\kappa} \varphi_\mu \varphi_\kappa$$

6gaa
$$C_{6gaa}^{(s)} = -\frac{48}{z^3} \sum_\mu^2 \sum_\kappa^2 \sum_\lambda^2 \frac{N_g}{M_\mu} \frac{N_a}{M_\kappa} \frac{N_a}{M_\lambda} \varphi_\mu \varphi_\kappa \varphi_\lambda - \frac{24}{z^3} \sum_\mu^2 \sum_\kappa^2 \frac{N_g}{M_\mu} \frac{N_a}{M_\kappa} \varphi_\mu \varphi_\kappa - \frac{6}{z^3} \sum_\mu^2 \sum_\kappa^2 \frac{N_l}{M_\mu} \frac{N_a}{M_\kappa} \varphi_\mu \varphi_\kappa$$

6ha $\quad C_{6ha}^{(s)} = \frac{6}{z^3} \sum_\mu^2 \sum_\kappa^2 \frac{N_h}{M_\mu} \frac{N_a}{M_\kappa} \varphi_\mu \varphi_\kappa$
 6ia $\quad C_{6ia}^{(s)} = \frac{2}{z^3} \sum_\mu^2 \sum_\kappa^2 \frac{N_i}{M_\mu} \frac{N_a}{M_\kappa} \varphi_\mu \varphi_\kappa$

6ja $\quad C_{6ja}^{(s)} = 0$
 6ka $\quad C_{6ka}^{(s)} = \frac{10}{z^3} \sum_\mu^2 \sum_\kappa^2 \frac{N_k}{M_\mu} \frac{N_a}{M_\kappa} \varphi_\mu \varphi_\kappa$

6la $\quad C_{6la}^{(s)} = \frac{18}{z^3} \sum_\mu^2 \sum_\kappa^2 \frac{N_l}{M_\mu} \frac{N_a}{M_\kappa} \varphi_\mu \varphi_\kappa$

6bbaa
$$C_{6bbaa}^{(s)} = \frac{106}{z^3} \sum_\mu^2 \sum_\kappa^2 \sum_\lambda^2 \sum_\tau^2 \frac{N_b}{M_\mu} \frac{N_b}{M_\kappa} \frac{N_a}{M_\lambda} \frac{N_a}{M_\tau} \varphi_\mu \varphi_\kappa \varphi_\lambda \varphi_\tau - \frac{8}{z^3} \sum_\mu^2 \sum_\kappa^2 \sum_\lambda^2 \frac{N_b}{M_\mu} \frac{N_b}{M_\kappa} \frac{N_a}{M_\lambda} \varphi_\mu \varphi_\kappa \varphi_\lambda$$
$$- \frac{8}{z^3} \sum_\mu^2 \sum_\kappa^2 \sum_\lambda^2 \frac{N_c}{M_\mu} \frac{N_b}{M_\kappa} \frac{N_a}{M_\lambda} \varphi_\mu \varphi_\kappa \varphi_\lambda - \frac{12}{z^3} \sum_\mu^2 \sum_\kappa^2 \sum_\lambda^2 \frac{N_d}{M_\mu} \frac{N_b}{M_\kappa} \frac{N_a}{M_\lambda} \varphi_\mu \varphi_\kappa \varphi_\lambda + \frac{4}{z^3} \sum_{\mu=1}^2 \sum_{\kappa=1}^2 \frac{N_b}{M_\mu} \frac{N_a}{M_\kappa} \varphi_\mu \varphi_\kappa$$
$$+ \frac{4}{z^3} \sum_{\mu=1}^2 \sum_{\kappa=1}^2 \frac{N_b}{M_\mu} \frac{N_b}{M_\kappa} \varphi_\mu \varphi_\kappa + \frac{14}{z^3} \sum_{\mu=1}^2 \sum_{\kappa=1}^2 \frac{N_c}{M_\mu} \frac{N_a}{M_\kappa} \varphi_\mu \varphi_\kappa + \frac{36}{z^3} \sum_{\mu=1}^2 \sum_{\kappa=1}^2 \frac{N_d}{M_\mu} \frac{N_a}{M_\kappa} \varphi_\mu \varphi_\kappa$$
$$+ \frac{14}{z^3} \sum_{\mu=1}^2 \sum_{\kappa=1}^2 \frac{N_e}{M_\mu} \frac{N_a}{M_\kappa} \varphi_\mu \varphi_\kappa + \frac{30}{z^3} \sum_{\mu=1}^2 \sum_{\kappa=1}^2 \frac{N_f}{M_\mu} \frac{N_a}{M_\kappa} \varphi_\mu \varphi_\kappa + \frac{96}{z^3} \sum_{\mu=1}^2 \sum_{\kappa=1}^2 \frac{N_g}{M_\mu} \frac{N_a}{M_\kappa} \varphi_\mu \varphi_\kappa$$
$$+ \frac{6}{z^3} \sum_\mu^2 \sum_\kappa^2 \frac{N_h}{M_\mu} \frac{N_a}{M_\kappa} \varphi_\mu \varphi_\kappa + \frac{8}{z^3} \sum_\mu^2 \sum_\kappa^2 \frac{N_i}{M_\mu} \frac{N_a}{M_\kappa} \varphi_\mu \varphi_\kappa + \frac{8}{z^3} \sum_\mu^2 \sum_\kappa^2 \frac{N_j}{M_\mu} \frac{N_a}{M_\kappa} \varphi_\mu \varphi_\kappa$$
$$+ \frac{10}{z^3} \sum_\mu^2 \sum_\kappa^2 \frac{N_k}{M_\mu} \frac{N_a}{M_\kappa} \varphi_\mu \varphi_\kappa + \frac{18}{z^3} \sum_\mu^2 \sum_\kappa^2 \frac{N_l}{M_\mu} \frac{N_a}{M_\kappa} \varphi_\mu \varphi_\kappa + \frac{8}{z^3} \sum_{\mu=1}^2 \sum_\kappa^2 \frac{N_c}{M_\mu} \frac{N_b}{M_\kappa} \varphi_\mu \varphi_\kappa$$
$$+ \frac{18}{z^3} \sum_{\mu=1}^2 \sum_{\kappa=1}^2 \frac{N_d}{M_\mu} \frac{N_b}{M_\kappa} \varphi_\mu \varphi_\kappa + \frac{2}{z^3} \sum_{\mu=1}^2 \sum_{\kappa=1}^2 \frac{N_d}{M_\mu} \frac{N_b}{M_\kappa} \varphi_\mu \varphi_\kappa + \frac{4}{z^3} \sum_{\mu=1}^2 \sum_{\kappa=1}^2 \frac{N_c}{M_\mu} \frac{N_c}{M_\kappa} \varphi_\mu \varphi_\kappa$$
$$+ \frac{9}{z^3} \sum_{\mu=1}^2 \sum_{\kappa=1}^2 \frac{N_d}{M_\mu} \frac{N_d}{M_\kappa} \varphi_\mu \varphi_\kappa + \frac{12}{z^3} \sum_{\mu=1}^2 \sum_{\kappa=1}^2 \frac{N_d}{M_\mu} \frac{N_c}{M_\kappa} \varphi_\mu \varphi_\kappa$$

6cba
$$C_{6cba}^{(s)} = -\frac{16}{z^3}\sum_{\mu}^{2}\sum_{\kappa}^{2}\sum_{\lambda}^{2}\frac{N_c}{M_\mu}\frac{N_b}{M_\kappa}\frac{N_a}{M_\lambda}\varphi_\mu\varphi_\kappa\varphi_\lambda \; -\frac{4}{z^3}\sum_{\mu=1}^{2}\sum_{\kappa=1}^{2}\frac{N_c}{M_\mu}\frac{N_a}{M_\kappa}\varphi_\mu\varphi_\kappa \; -\frac{4}{z^3}\sum_{\mu=1}^{2}\sum_{\kappa=1}^{2}\frac{N_e}{M_\mu}\frac{N_a}{M_\kappa}\varphi_\mu\varphi_\kappa$$

$$-\frac{8}{z^2}\sum_{\mu=1}^{2}\sum_{\kappa=1}^{2}\frac{N_f}{M_\mu}\frac{N_a}{M_\kappa}\varphi_\mu\varphi_\kappa \; -\frac{4}{z^3}\sum_{\mu}^{2}\sum_{\kappa}^{2}\frac{N_h}{M_\mu}\frac{N_a}{M_\kappa}\varphi_\mu\varphi_\kappa \; -\frac{2}{z^3}\sum_{\mu}^{2}\sum_{\kappa}^{2}\frac{N_i}{M_\mu}\frac{N_a}{M_\kappa}\varphi_\mu\varphi_\kappa$$

$$-\frac{4}{z^3}\sum_{\mu}^{2}\sum_{\kappa}^{2}\frac{N_j}{M_\mu}\frac{N_a}{M_\kappa}\varphi_\mu\varphi_\kappa \; -\frac{6}{z^3}\sum_{\mu}^{2}\sum_{\kappa}^{2}\frac{N_l}{M_\mu}\frac{N_a}{M_\kappa}\varphi_\mu\varphi_\kappa \; -\frac{4}{z^3}\sum_{\mu=1}^{2}\sum_{\kappa=1}^{2}\frac{N_c}{M_\mu}\frac{N_c}{M_\kappa}\varphi_\mu\varphi_\kappa$$

$$-\frac{2}{z^3}\sum_{\mu=1}^{2}\sum_{\kappa=1}^{2}\frac{N_c}{M_\mu}\frac{N_b}{M_\kappa}\varphi_\mu\varphi_\kappa \; -\frac{6}{z^3}\sum_{\mu=1}^{2}\sum_{\kappa=1}^{2}\frac{N_d}{M_\mu}\frac{N_c}{M_\kappa}\varphi_\mu\varphi_\kappa$$

6dba
$$C_{6dba}^{(s)} = \frac{120}{z^3}\sum_{\mu}^{2}\sum_{\kappa}^{2}\sum_{\lambda}^{2}\frac{N_d}{M_\mu}\frac{N_b}{M_\kappa}\frac{N_a}{M_\lambda}\varphi_\mu\varphi_\kappa\varphi_\lambda - \frac{18}{z^3}\sum_{\mu=1}^{2}\sum_{\kappa=1}^{2}\frac{N_d}{M_\mu}\frac{N_a}{M_\kappa}\varphi_\mu\varphi_\kappa \; -\frac{6}{z^3}\sum_{\mu=1}^{2}\sum_{\kappa=1}^{2}\frac{N_f}{M_\mu}\frac{N_a}{M_\kappa}\varphi_\mu\varphi_\kappa$$

$$-\frac{72}{z^2}\sum_{\mu=1}^{2}\sum_{\kappa=1}^{2}\frac{N_g}{M_\mu}\frac{N_a}{M_\kappa}\varphi_\mu\varphi_\kappa \; -\frac{6}{z^3}\sum_{\mu=1}^{2}\sum_{\kappa=1}^{2}\frac{N_i}{M_\mu}\frac{N_a}{M_\kappa}\varphi_\mu\varphi_\kappa \; -\frac{12}{z^3}\sum_{\mu}^{2}\sum_{\kappa}^{2}\frac{N_k}{M_\mu}\frac{N_a}{M_\kappa}\varphi_\mu\varphi_\kappa$$

$$-\frac{6}{z^3}\sum_{\mu}^{2}\sum_{\kappa}^{2}\frac{N_l}{M_\mu}\frac{N_a}{M_\kappa}\varphi_\mu\varphi_\kappa \; -\frac{6}{z^3}\sum_{\mu=1}^{2}\sum_{\kappa=1}^{2}\frac{N_d}{M_\mu}\frac{N_b}{M_\kappa}\varphi_\mu\varphi_\kappa \; -\frac{18}{z^3}\sum_{\mu=1}^{2}\sum_{\kappa=1}^{2}\frac{N_d}{M_\mu}\frac{N_d}{M_\kappa}\varphi_\mu\varphi_\kappa$$

$$-\frac{12}{z^3}\sum_{\mu=1}^{2}\sum_{\kappa=1}^{2}\frac{N_d}{M_\mu}\frac{N_c}{M_\kappa}\varphi_\mu\varphi_\kappa$$

6eb
$$C_{6eb}^{(s)} = \frac{4}{z^3}\sum_{\mu=1}^{2}\sum_{\kappa=1}^{2}\frac{N_e}{M_\mu}\frac{N_b}{M_\kappa}\varphi_\mu\varphi_\kappa$$

6fb
$$C_{6fb}^{(s)} = -\frac{6}{z^3}\sum_{\mu=1}^{2}\sum_{\kappa=1}^{2}\frac{N_f}{M_\mu}\frac{N_b}{M_\kappa}\varphi_\mu\varphi_\kappa + \frac{4}{z^3}\sum_{\mu=1}^{2}\frac{N_f}{M_\mu}\varphi_\mu + \frac{1}{z^3}\sum_{\mu=1}^{2}\frac{N_i}{M_\mu}\varphi_\mu + \frac{2}{z^3}\sum_{\mu=1}^{2}\frac{N_j}{M_\mu}\varphi_\mu + \frac{8}{z^3}\sum_{\mu=1}^{2}\frac{N_k}{M_\mu}\varphi_\mu + \frac{9}{z^3}\sum_{\mu=1}^{2}\frac{N_l}{M_\mu}\varphi_\mu$$

$$+\frac{1}{z^3}\sum_{\mu=1}^{2}\frac{N_n}{M_\mu}\varphi_\mu + \frac{1}{z^3}\sum_{\mu=1}^{2}\frac{N_o}{M_\mu}\varphi_\mu + \frac{1}{z^3}\sum_{\mu=1}^{2}\frac{N_p}{M_\mu}\varphi_\mu + \frac{2}{z^3}\sum_{\mu=1}^{2}\frac{N_q}{M_\mu}\varphi_\mu + \frac{2}{z^3}\sum_{\mu=1}^{2}\frac{N_s}{M_\mu}\varphi_\mu + \frac{3}{z^3}\sum_{\mu=1}^{2}\frac{N_t}{M_\mu}\varphi_\mu$$

6gb
$$C_{6gb}^{(s)} = -\frac{12}{z^3}\sum_{\mu=1}^{2}\sum_{\kappa=1}^{2}\frac{N_g}{M_\mu}\frac{N_b}{M_\kappa}\varphi_\mu\varphi_\kappa + \frac{18}{z^3}\sum_{\mu=1}^{2}\frac{N_g}{M_\mu}\varphi_\mu + \frac{3}{z^3}\sum_{\mu=1}^{2}\frac{N_l}{M_\mu}\varphi_\mu + \frac{3}{z^3}\sum_{\mu=1}^{2}\frac{N_r}{M_\mu}\varphi_\mu + \frac{3}{z^3}\sum_{\mu=1}^{2}\frac{N_t}{M_\mu}\varphi_\mu$$

6bbb
$$C_{6bbb}^{(s)} = -\frac{16}{3z^3}\sum_{\mu}^{2}\sum_{\kappa}^{2}\sum_{\lambda}^{2}\frac{N_b}{M_\mu}\frac{N_b}{M_\kappa}\frac{N_b}{M_\lambda}\varphi_\mu\varphi_\kappa\varphi_\lambda + \frac{2}{z^3}\sum_{\mu=1}^{2}\sum_{\kappa=1}^{2}\frac{N_b}{M_\mu}\frac{N_b}{M_\kappa}\varphi_\mu\varphi_\kappa + \frac{4}{z^3}\sum_{\mu=1}^{2}\sum_{\kappa=1}^{2}\frac{N_c}{M_\mu}\frac{N_b}{M_\kappa}\varphi_\mu\varphi_\kappa + \frac{12}{z^3}\sum_{\mu=1}^{2}\sum_{\kappa=1}^{2}\frac{N_d}{M_\mu}\frac{N_b}{M_\kappa}\varphi_\mu\varphi_\kappa$$

$$+\frac{4}{z^3}\sum_{\mu=1}^{2}\sum_{\kappa=1}^{2}\frac{N_e}{M_\mu}\frac{N_b}{M_\kappa}\varphi_\mu\varphi_\kappa + \frac{4}{z^3}\sum_{\mu=1}^{2}\sum_{\kappa=1}^{2}\frac{N_f}{M_\mu}\frac{N_b}{M_\kappa}\varphi_\mu\varphi_\kappa + \frac{12}{z^3}\sum_{\mu=1}^{2}\sum_{\kappa=1}^{2}\frac{N_g}{M_\mu}\frac{N_b}{M_\kappa}\varphi_\mu\varphi_\kappa - \frac{1}{3z^3}\sum_{\mu=1}^{2}\frac{N_b}{M_\mu}\varphi_\mu$$

$$-\frac{2}{z^3}\sum_{\mu=1}^{2}\frac{N_c}{M_\mu}\varphi_\mu - \frac{8}{z^3}\sum_{\mu=1}^{2}\frac{N_d}{M_\mu}\varphi_\mu - \frac{4}{z^3}\sum_{\mu=1}^{2}\frac{N_e}{M_\mu}\varphi_\mu - \frac{8}{z^3}\sum_{\mu=1}^{2}\frac{N_f}{M_\mu}\varphi_\mu - \frac{38}{z^3}\sum_{\mu=1}^{2}\frac{N_g}{M_\mu}\varphi_\mu - \frac{2}{z^3}\sum_{\mu=1}^{2}\frac{N_h}{M_\mu}\varphi_\mu$$

$$-\frac{5}{z^3}\sum_{\mu=1}^{2}\frac{N_i}{M_\mu}\varphi_\mu - \frac{4}{z^3}\sum_{\mu=1}^{2}\frac{N_j}{M_\mu}\varphi_\mu - \frac{8}{z^3}\sum_{\mu=1}^{2}\frac{N_k}{M_\mu}\varphi_\mu - \frac{12}{z^3}\sum_{\mu=1}^{2}\frac{N_l}{M_\mu}\varphi_\mu - \frac{1}{z^3}\sum_{\mu=1}^{2}\frac{N_m}{M_\mu}\varphi_\mu - \frac{1}{z^3}\sum_{\mu=1}^{2}\frac{N_n}{M_\mu}\varphi_\mu$$

$$-\frac{1}{z^3}\sum_{\mu=1}^{2}\frac{N_o}{M_\mu}\varphi_\mu - \frac{1}{z^3}\sum_{\mu=1}^{2}\frac{N_p}{M_\mu}\varphi_\mu - \frac{1}{z^3}\sum_{\mu=1}^{2}\frac{N_q}{M_\mu}\varphi_\mu - \frac{3}{z^3}\sum_{\mu=1}^{2}\frac{N_r}{M_\mu}\varphi_\mu - \frac{2}{z^3}\sum_{\mu=1}^{2}\frac{N_s}{M_\mu}\varphi_\mu - \frac{9}{z^3}\sum_{\mu=1}^{2}\frac{N_t}{M_\mu}\varphi_\mu$$

$$-\frac{2}{z^3}\sum_{\mu=1}^{2}\frac{N_u}{M_\mu}\varphi_\mu$$

6cc
$$C_{6cc}^{(s)} = \frac{4}{z^3}\sum_{\mu=1}^{2}\sum_{\kappa=1}^{2}\frac{N_c}{M_\mu}\frac{N_c}{M_\kappa}\varphi_\mu\varphi_\kappa$$

6dc
$$C_{6cd}^{(s)} = \frac{6}{z^3}\sum_{\mu=1}^{2}\sum_{\kappa=1}^{2}\frac{N_d}{M_\mu}\frac{N_c}{M_\kappa}\varphi_\mu\varphi_\kappa$$

6dd
$$C_{6dd}^{(s)} = \frac{9}{z^3}\sum_{\mu=1}^{2}\sum_{\kappa=1}^{2}\frac{N_d}{M_\mu}\frac{N_d}{M_\kappa}\varphi_\mu\varphi_\kappa$$

4 Results

The Lattice Cluster Theory in its original form (1) can describe the properties of long chain molecules well. For this it requires only one parameter set for all possible isomers of a molecule, which describes their properties. This proves to be very advantageous because many isomers are difficult to separate due to their similar chemical and thermodynamic properties. In the case of smaller molecules, this form reaches its limits. It can hardly distinguish between the individual isomers of small molecules. The extensions to the model made in this work should improve the applicability in these cases.

In order to recognize the effects of the extension, exactly such components are therefore to be investigated. Pentane (17) (18) (19) (20) (21), hexane (17) (22) and octane (17) (20) are investigated. For pentane, the components examined are n-pentane and 2,2-dimethylbutane. All three were calculated with the same parameter set, which was fitted to the n-pentane. For hexane, the isomers are n-hexane, .2-methylpentane, 3-methylpentane, 2,2-dimethylbutane, 2,3-dimethylbutane. Here the parameter set was created with n-hexane. The three isomers studied from octane are n-octane and 3-methylheptane. As with the other components, the unbranched isomer was used to create the parameter set. The unbranched isomers were chosen because they are the simplest to isolate. The experimental determination of their material data is therefore the least problematic.

The vapour pressure and the liquid density are used as substance properties to adjust the parameter set. The vapour pressure of the component is derived from the expression Eq. 4.1. By inserting the normalized free Helmholtz energy and substituting n_μ with the volume fraction, the expression becomes Eq. 4.2. The density of the liquid phase can be described by the expression Eq. 4.3.

$$-p = \left(\frac{\partial F}{\partial V}\right)_{n_i,T}$$

Eq. 4.1

$$p = -\frac{1}{\sigma^3} * \left(f - \varphi_i * \frac{\partial f}{\partial \varphi_i}\right)$$

Eq. 4.2

$$\rho_l = \frac{\varphi_i}{\sigma^3} * \frac{MM_i}{N_A}$$

Eq. 4.3

In Table 7 the substance properties used for the generation are listed. This parameter set is then used to calculate the other isomers. For the calculation of the substance data the individual isomers differ only in the frequency N_i of the diagram in the molecule . This indicates how often the respective structure is found in a molecule. To satisfy the model equations, the thermodynamic equilibrium conditions of pressure and chemical potential are solved. The pressure is solved again with the expression Eq. 4.2. For the chemical potential, the expression Eq. 4.4 is used, which becomes Eq. 4.5 by substituting the individual variables.

$$\mu_i = \left(\frac{\partial F}{\partial n_i}\right)_{V,T}$$

Eq. 4.4

$$\mu_i = f + (1 - \varphi_i) * \frac{\partial f}{\partial \varphi_i}$$

Eq. 4.5

Table 7: Experimental data of the isomers used for the parameter fitting

n-Alkanes	Temperature [K]	Pressure [Pa]	Liquid density [kg/m³]	Reference
n-Pentane	197	133.3		(23)
	223.1	1333		
	260.6	13330		
	273.15		719.4	
	293.15		704.2	
	313.15		684.9	
n-Hexane	219.3	133.3		(23)
	289	13330		
	341.9	101300		
	343.15		611.2	
	423.15		519.1	
	503.15		332.7	
n-Octane	259.2	133.3		(23) (24)
	292.4	1333		
	338.9	13330		
	273.15		719.42	
	293.15		704.23	
	333.15		671.14	

The modified LCT is compared with the underlying versions of Freed (1) and Zimmermann (6). Thereby the effects of the diagrams with six bonds shall be observed. Since the modified LCT considers the term of energy with the energetic mean field alone, this term is also applied to the other versions for a better comparison of the models. All energetic diagrams, which are not included in the energetic mean field, are neglected. Three different versions of the new modified LCT were considered and

compared with two modified versions by Zimmermann (6) and the original modified LCT (1). These inspected models are listed in.

Table 8 : All inspected cases of the model in the thesis

	max. contribution of diagram	max. number of bonds	Reference
Case 1	$\varepsilon^3 z^{-3}$	6	
Case 2	$\varepsilon^2 z^{-3}$	6	
Case 3	$\varepsilon\, z^{-3}$	6	
Case 4	$\varepsilon^2 z^{-3}$	4	Zimmermann et al. (6)
Case 5	$\varepsilon\, z^{-3}$	4	Zimmermann et al. (6)
Case 6	$\varepsilon^2 z^{-2}$	4	Freed et al. (1)

For some inspected cases and corresponding component, a set of parameters is fitted. All three parameter, Side length of lattice cell σ, Interaction parameter $\varepsilon_{ii,1}$ and Interaction parameter $\varepsilon_{ii,2}$, are listed in Table 9.

Table 9 : The parameter sets of Pentane, Hexane and Octane used for LCT

Component	Model	σ [Å]	$\varepsilon_{ii,1}$	$\varepsilon_{ii,2}$
Pentane	Case 1	2.89364	116.463	254.936
	Case 4	2.91483	84.3035	496.323
	Case 6	2.93205	81.1779	523.992
Hexane	Case 1	2.83018	105.911	310.068
	Case 2	2.90800	64.8938	726.101
	Case 3	3.31947	89.2108	238.997
	Case 4	2.90063	80.8263	535.401
	Case 5	3.21217	109.064	196.451
	Case 6	2.90928	80.1492	539.923
Octane	Case 1	2.68332	94.2913	399.333
	Case 4	2.63272	131.629	244.981
	Case 6	2.75725	72.8886	652.756

By directly comparing the calculated vapour pressures for the isomers of hexane with the experimental data, their modelability with the different models can be illustrated. Figure 10, Figure 11 and Figure 12 show the vapor pressures in the range 200 to 350 K for all five isomers. Here all three possibilities for modelling the energetic mean field were compared. In all three cases the curve of the n-hexane deviates only slightly from the experimental values. This is explained by the fact that the parameter set was fitted with n-hexane. For the remaining isomers there is an increasing deviation of the curves from the experimental data. It can be observed that with increasing deviation of the experimental values from the values of the n-hexane, the deviation of the model also increases. The calculated vapour pressures of the isomers decrease while the experimental ones increase. This results in an inverse order of the vapour pressures. Only the two isomers 2-methylpentane and 3-methylpentane are shown in the correct order. This effect is strongest in the model which represents the energetic part, only with the χ function, which corresponds to a maximum contribution of $\varepsilon\,z^{-3}$.

With the increase of the ε exponent and thus included diagrams the error decreases. When directly comparing the modelling of the hexane isomers with the adapted form of the Freed Model in Figure 10 with the newly extended form ε^3z^{-3} in Figure 9, the former hardly distinguishes between the isomers. The results of the model according to Freed (1) all clearly follow the results for the n-hexane, which was used to fit the parameters.
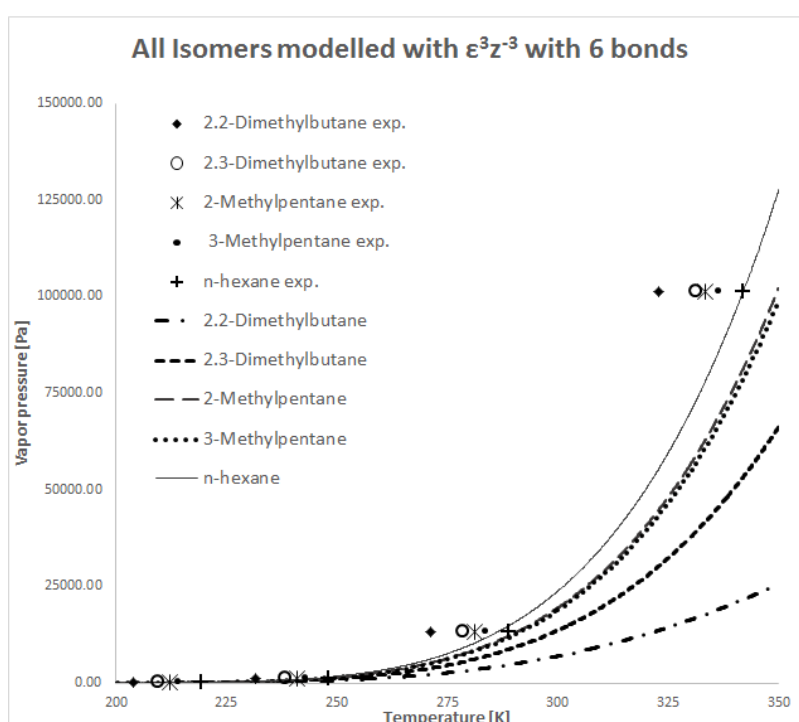
Figure 9: The vapor pressure of all isomers of hexane calculated with the modified model with six bonds and ε^3z^{-3} (23) (25)
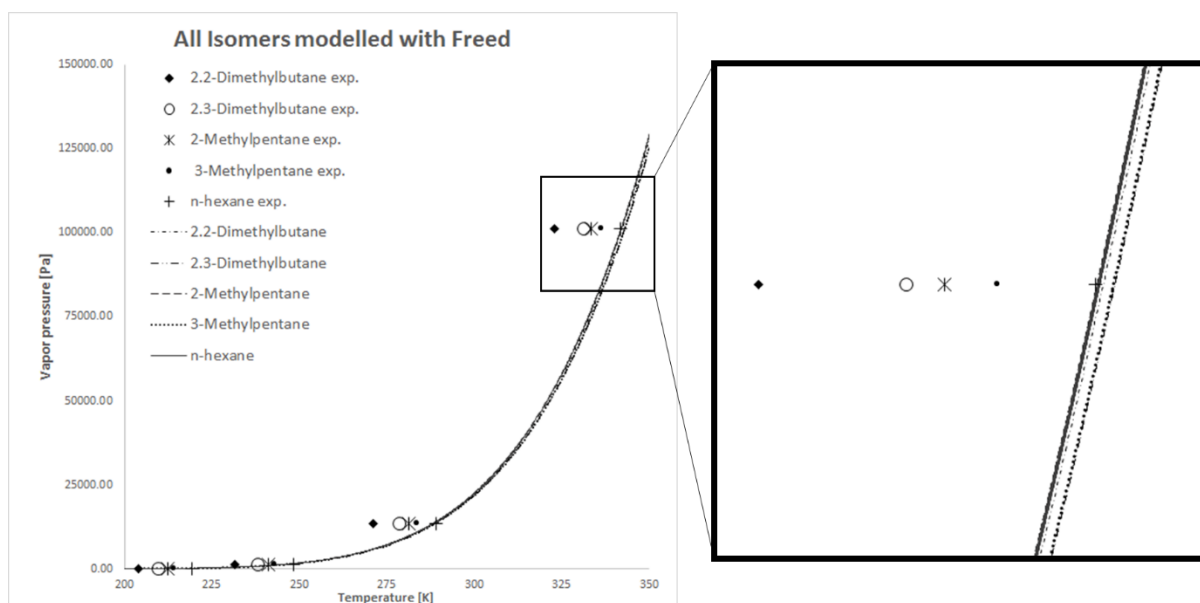
Figure 10: The vapor pressure of all isomers of hexane calculated with the modified model according to Freed (1) (23) (25)
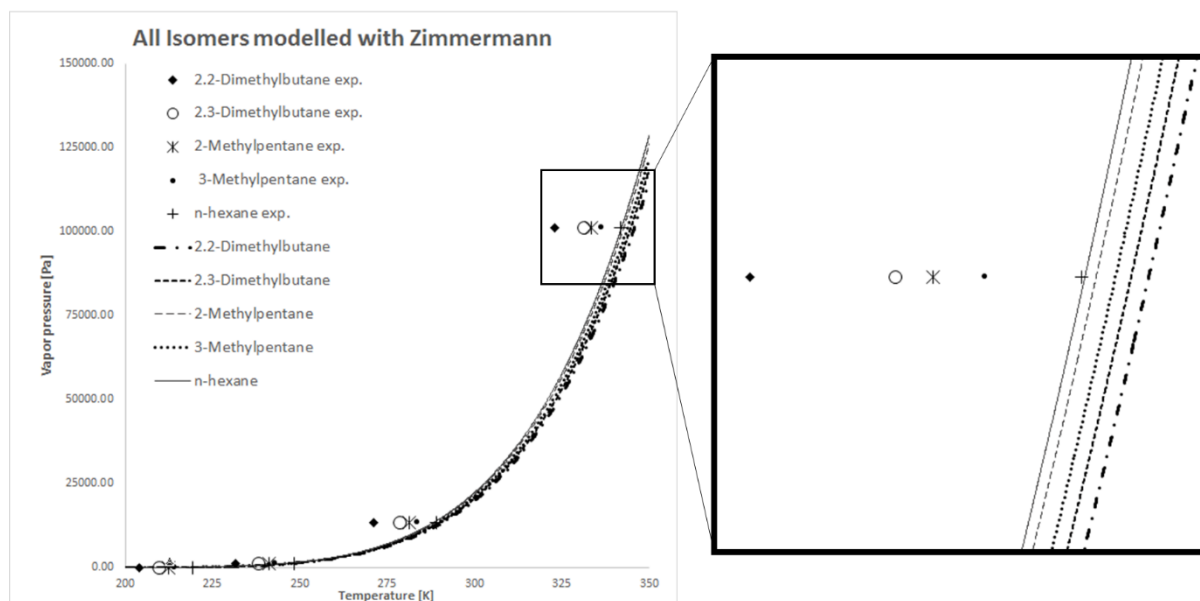
Figure 11: The vapor pressure of all isomers of hexane calculated with the modified model according to Zimmermann (6) (23) (25)
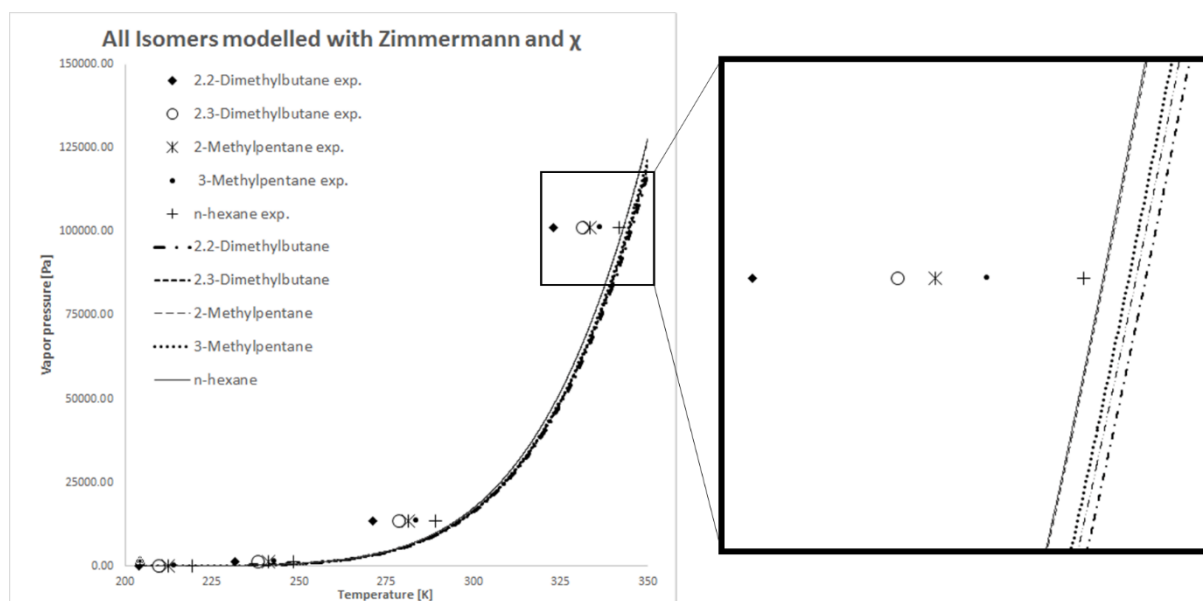
Figure 12: The vapor pressure of all isomers of hexane calculated with the modified model according to Zimmermann with the energetic contribution described with the chi-function (6) (23) (25)

As with the results of the extended models, there is a deviation of the results in the wrong direction. It has a much smaller error than the extended model, but its results differ less. When increasing the resolution by the range of 10 000 Pascal it becomes clear that the order is reversed in the same way as with the other models.

The modified form of the model developed by Zimmermann (6) with a maximum contribution of $\varepsilon^2 z^{-3}$ and diagram with up to four bonds can distinguish more clearly between the individual isomers when calculating the vapour pressure curve. However, like the other models, it also deviates in the wrong direction. The resulting error is considerably larger than that of the modified Freed model, but smaller than the error of the extended model. In the comparison, the error of model of Zimmermann et al. (6) version with the χ-function for the energy terms is noticeably larger.

The direct comparison of the vapour pressure curves of the isomer 2,2-dimethylbutane is shown in Figure 13 for all models considered. Here it is clearly visible that the deviation from the experimental data is smallest for the modified model of Freed, followed by the modified model of Zimmermann, the extended model with a maximum contribution of $\varepsilon^3 z^{-3}$, the one with a maximum contribution of $\varepsilon^2 z^{-3}$ and the one using the χ-function. For all models, the error also increased significantly with increasing temperature. The relative error on the other hand decreases for models according to Freed (1) and Zimmermann (6) and is relative constant for the expanded models. This can be seen in Figure 14.
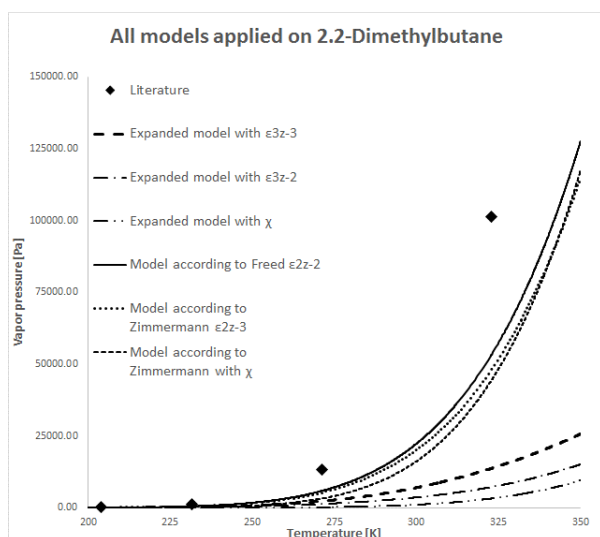
Figure 13: The vapor pressure of 2.2-Dimethylbutane calculated with all inspected models (23)
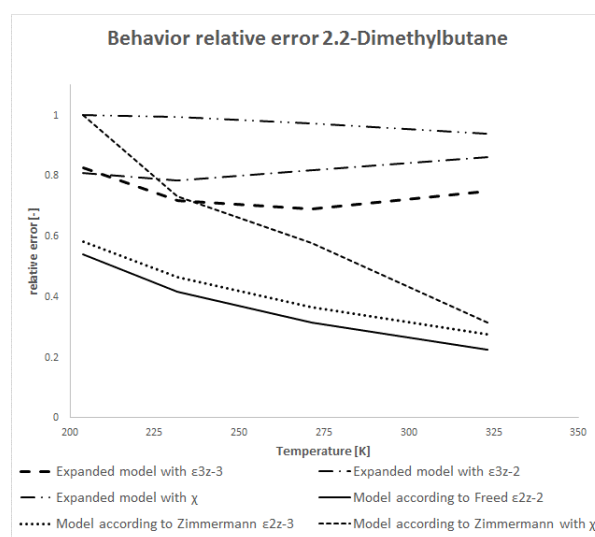
Figure 14: The behavior of the relative error for all models for 2,2-Dimethylbutane

The same trend in predictive power can be observed in the Figure 16 and Figure 15 for isomers 2.2 dimethylpropane and 3-methylheptane. Here it can also be observed that the behaviour also occurs at the lower temperatures with 2.2-dimethylpropane.

When comparing the vapour pressure curves for the isomer n-hexane, which was used for the creation of the parameter sets, almost all curves can follow the experimental data well. Only the models using the χ function deviate slightly from the data sets.
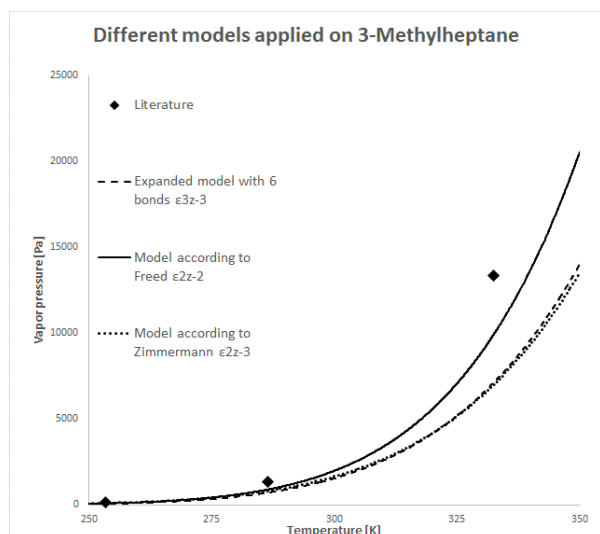
Figure 15: The vapor pressure of 3-Methylheptane calculated with the adjusted models according to Freed and Zimmermann as well as with expanded model (23)
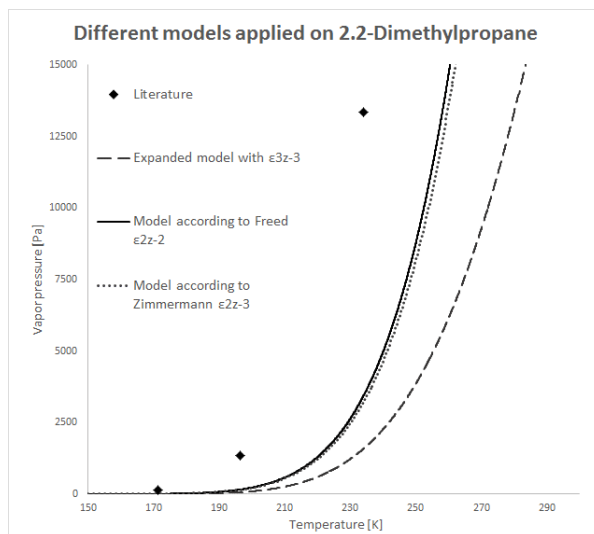
Figure 16:The vapor pressure of 2.2-Dimethylpropane calculated with the adjusted models according to Freed and Zimmermann as well as with expanded model (20) (23) (26)

5 Interpretation

The results of the individual models show that the new extended models have a larger error than the previous models. This can lead to the conclusion that the underlying assumption of the work is incorrect. An extension of the entropic diagrams to diagrams with up to six bonds does not increase the predictive power of LCT for small molecules. It even leads to a deterioration of the predictive power. However, the fact that none of the considered models with the energetic mean field alone can correctly predict the sequence must also be taken into account. According to Zimmermann (6) his model with a contribution of $\varepsilon^2 z^{-3}$ is largely able to represent the vapour pressures in the correct order. In this case, the deviation that increases with temperature can be explained by the neglection of the energy diagrams. This is also supported by the fact that the additional omission of the diagrams with ε^2 leads to a further shift of the vapor pressure curves in the wrong direction. This is also supported by the observation that the error of the extended models increases with less energy diagrams considered. The error may therefore be due to neglecting the energetic diagrams. The diagrams which include both bonds and interactions. The assumption that entropic diagrams and the energetic mean field are sufficient to detect an improvement of the modelability of small molecules can be rejected.

The energetic diagrams additionally introduce a multitude of terms with ε of different orders. Since the interaction parameter is a function of temperature, as can be seen with the function Eq. 3.59, these diagrams bring with them an additional temperature dependence. Their omission can partly explain the temperature dependence of the error.

When considering the fitted parameters for the individual models in Table 9 the lattice size σ decreases with increasing molecule size. However, the individual segments of the components are quite similar. This would correspond to a similar grid size. In the case of the models under consideration, the parameters possibly compensate for the errors caused by the missing energy dependencies. Especially for diagrams with larger molecules the mean field is no longer sufficient, and the error is compensated by the parameters.

Compared to Freed, the extended models are also able to distinguish clearly between the individual isomers. While the structure of the isomers has only a minimal influence on the modelability in the former versions, is the influence clearly visible in

the extended models. With the extended LCT the structure of the small molecules has an influence on the calculated results. Without considering the remaining energetic diagrams it cannot be determined whether the extension has a better predictive power for small molecules.

The next considered step to improve the model would therefore be the development of the energetic diagrams up to a contribution from $\varepsilon^3 z^{-3}$.

6 Summary

Current forms of LCT are already well suited for modelling large molecules such as polymers. However, in the area of smaller molecules, such as hexane, it is not really able to distinguish between the individual isomers. This limits their applicability for many systems. The introduction of diagrams with up to six bonds should make it possible to distinguish between the individual isomers of these components. For this purpose, 46 new entropic diagrams have been introduced, 14 that consist of a single structure and 32 diagrams that consist of multiple structures. When calculating their contributions, the lattice-dependent and the combinatorial components were determined separately. For the lattice-dependent contribution only contributions with a z-exponent of at least z^{-3} were considered. Contributions with a lower order were neglected. In addition, the methodology for determining the number of ways to contract a diagram has been standardized. For the combinatorial contribution of the individual diagrams the counting methodology introduced by Nemirovsky (15) is used. This leads to the omission of diagrams which correct errors in the previous counting method. However, it leads to the introduction of so-called correction diagrams (CorD) in the combinatorial part. Each of these has a pre-factor for which a method for determination is found. The energetic diagrams of the LCT are presented with the energetic mean field. This contains only energetic diagrams, which consist exclusively of interaction bonds. In order to observe the effects of omitting the remaining energetic diagrams, the mean field is described by different numbers of diagrams. The extended LCT thus has a maximum contribution of $\varepsilon^{3}z^{-3}$. When calculating the vapour pressures of the isomers of pentane, hexane and octane, one obtains clearly different results for the individual isomers. When comparing with the current form of the LCT, where the energy is also expressed only by the mean field, the error for the expanded form is larger for the individual isomers. Their results deviate more from the experimental data. When looking at the influence of the energetic diagrams, it becomes clear that this can be explained by omitting most of them. The next step in the extension of the LCT would be the inclusion of all these energetic diagrams.

7 Appendix

7.1 Symbols

Variables

C_i	Contribution of a diagram
D_B	Lattice dependent contribution
d_B	Enumerator of lattice dependent contribution
e	energetic contribtion
F	Helmholtz energy [J]
f	Normalized Helmholtz energy [J/segment]
f_1	First binomial coefficiant for α
f_2	Second binomial coefficiant for α
$f_{B,c}$	Pre-factor for contracted diagram
f_{cd}	Pre-factor for formable correction diagrams
$f_{cd,i}$	Pre-factor of correction diagram from diagram i
f_{cu}	Pre-factor for cumulants
f_{eq}	Pre-factor for equal structures
f_{ii}	Mayer- f function
k	Number of components
k_B	Boltzmann constant [J/K]
k_i	Number of merged vertices on choosen vertex
k_{ln}	Coefficient of cumulant deriving from series development
M_i	Number of segments in molecule
MM	Molare mass [kg/mol]
$N\grave{}_v$	Number of vertices in contracted diagram
N_A	Avogadro constant [1/mol]
$n_{B,m}$	Number of ways to arrange vertices in contracted diagram

n_d	Number of different diagrams in cumulant
n_{df}	Number of the most common diagram in cummulant
n_{df2}	Number of the second most common diagram
n_μ	Number of molecules
N_i	Number of possible ways to place structure in the chain
$N_{i,j}$	Number of of positions lost in j through i
N_l	Number of lattice sides
n_o	Number of ways to place the similar structure
n_p	Number of states a structure can take in one position
n_{pos}	Number of identical positions
N_v	Number of vertices in cluster diagram
p	Pressure [Pa]
r	Position vector of lattice side
$R_{B,c}$	Contribution of the contracted diagram
S	Entropy [J/K]
s	Number of symmetries in appearance
s_D	Symmetry number
T	Temperature [K]
Z	Sum of states
z	Lattice coordination number
α	Denominator of lattice dependent contribution
α_i	Position vector to neighbor side
γ_D	Number of ways to choose the segments
γ_i	Combinatoral contribution
ε_{ii}	Interaction parameter for Interaction energy
$\varepsilon_{ii,1}$	Parameter 1 for the interaction parameter
$\varepsilon_{ii,2}$	Parameter 2 for the interaction parameter

μ_i	chemical potential [J/mol]
ρ_l	Density of liquid phase [kg/m3]
σ	Side length of one lattice cell [Angstrom]
ϕ_i	Volume fraction of component

Subscripts and superscripts

i	Placeholder for other index
μ; κ; λ; τ; ω; υ	Counter for the components
a…u	Respective structure
S	Volume contraction condition
m_i	Counter for molecules of one component
α_i	Counter for Segments in one molecule
β_i	Counter for all directions of lattice
MF	mean field
B,m	entropic diagram
B,e	energetic diagram
ε	order of energetic contribution
m	counter of bonds in contracted diagram
$i_1 \dots i_m$	counter for sides of lattice
j	counter for structures
l	counter for structures in contracted diagram
k	counter for positions in appearance
ax	counter of symmetry axis
CorD	Correction diagram
χ	chi function to model energy
V	constant volume

7.2   Bibliographie

1. **Freed, K.F.** New lattice model for interacting, avoiding polymers with controlled length distribution. *Journal of Physics A: Mathematical and General.* 1985, S. 871.

2. **Dudowicz, J, Freed, K.F. und Madden, W.G.** Role of molecular structure on the thermodynamic properties of melts, blends, and concentrated polymer solutions: comparison of Monte Carlo simulations with the cluster theory for the lattice model. *Macromolecules.* 1990, S. 4803-4819.

3. **Dudowicz, J und Freed, K.F.** Effect of monomer structure and compressibility on the properties of multicomponent polymer blends and solutions: 1. Lattice cluster theory of compressible systems. *Macromolecules.* 1991, S. 5076-5095.

4. **Dudowicz, J, Freed, K.F. und Douglas, J.F.** Modification of the phase stability of polymer blends by diblock copolymer additives. *Macromolecules.* 1995, S. 2276-2287.

5. **Zeiner, T, et al.** Calculation of the (liquid+ liquid) equilibrium of solutions of hyperbranched polymers with the lattice-cluster theory combined with an association model. *The Journal of Chemical Thermodynamics.* 2011, S. 1969-1976.

6. **Zimmermann, P, Walowski, C und Enders, S.** Impact of higher order diagrams on phase equilibrium calculations for small molecules using lattice cluster theory. *The Journal of Chemical Physics.* 2018, S. 094103.

7. **Esteban, S.** Liebig-Wöhler Controversy and the Concept of Isomerism. *Journal of Chemical Edurcation.* 2008, S. 1201-1203.

8. **Bailey, WM. A, et al.** Urea extractive crystallization of straight-chain hydrocarbons. *Industrial & Engineering Chemistry.* 1951, S. 2125-2129.

9. **Bytautas, L und Klein, D.J.** Chemical Combinatorics for Alkane-Isomer Enumeration and More. *Journal of chemical information and computer sciences.* 1998, S. 1063-1078.

10. **Flory , P. J.** *Principles of Polymer Chemistry.* Ithaca, NY : Cornell University Press, 1953.

11. **Mayer, J.E und Mayer, M.G.** *Statistical mechanics.* New York : Wiley, 1940.

12. **Langenbach, K und Enders, S.** Development of an EOS based on lattice cluster thoery for pure components. *Fluid Phase Equilibria.* 2012, S. 58-79.

13. **Brazhnik, O.D und Freed, K.F.** Application of graph theory to the statistical thermodynamics of lattice polymers. I.Elements of theory and test for dimers. *The Journal of Chemical Physics.* 1996, S. 837-861.

14. **Favre, Henri A und Powell, Warren H.** *Nomenclature of Organic Chemistry - IUPAC Recommendations and Preferred Names 2013.* s.l. : The Royal Society of Chemistry, 2014.

15. **Nemirovsky, A.M, Dudowicz, J und Freed, K.F.** Dense self-interacting lattice trees with specified topologies: From light to dense branching. *Physical Review A.* 1992, S. 7111.

16. **Foreman, K.W und Freed, K.F.** Lattice Cluster Theorie. *Advances in Chemical Physics.* 1998, S. 355.

17. **Dykyj, J, et al.** Vapor pressure of chemicals:Vapor pressure and Antoine constants for hydrocarbons, and S,Se,Te, and halogen containing organic compounds. *Landolt-Börnstein-Group IV Physical Chemistry, edited by K.R. Hall (Springer).* 1999.

18. **Osborn, A.G und Douslin, D.R.** Vapor-Pressure Relations for 15 Hydrocarbons. *Journal of Chemical and Engineering Data.* 1974, S. 114-117.

19. **Willingham, C.B, et al.** Vapor pressure and boiling points of some paraffin, alkylcyclohexane, and alkylbenzene hydrocarbons. *Journal of Research of the National Bureau of Standards.* 1945, S. 219-244.

20. **Ewing, M.B und Sanchez Ochoa, J.C.** Vapour pressures of n-hexane determined by comparative ebuliometry. *The Journal of Chemical Thermodynamics.* 2006, S. 283-288.

21. **Das, T.R, Reed, C.O und Eubank, P.T.** PVT surface and thermodynamic properties of n-pentane. *Journal of Chemical and Enigneering Data.* 1977, S. 3-9.

22. **Young, S.** The specific volumes of the saturated vapours of pure substances. *Zeitschrift für Physikalische Chemie.* 1910, S. 620-626.

23. **Landolt, Hans Heinrich und Börnstein, Richard.** *Physikalisch-chemische Tabellen.* s.l. : Springer Nature, 1992.

24. **Landolt, Hans Heinrich und Börnstein, Richard.** *Physikalisch-chemische Tabellen.* s.l. : Springer Nature, 1996.

25. **Goetsch, T, et al.** Liquid-Liquid Equilibrium and Interfacial Tension of Hexane Isomers-Methanol Systems. *Industrial & Engineering Chemistry Research.* 2017, S. 9743-9752.

26. **Das, T R, Reed, C O und Eubank, P T.** PVT surface and thermodynamic properties of n-pentane. *Journal of Chemical and Engineering Data.* 1977.

7.3   Figures

7.4   Tables